Theoretical Analysis of Spectra of Short Polyenes

GIORGIO ORLANDI,*,† FRANCESCO ZERBETTO,† and MAREK Z. ZGIERSKI*,‡

Dipartimento di Chimica "G. Ciamician", Università di Bologna, 40126 Bologna, Italy, and Steacie Institute for Molecular Sciences, National Research Council of Canada, Ottawa, K1A 0R6 Canada

Received March 25, 1991 (Revised Manuscript Received May 14, 1991)

Contents

1. Introduction

Polyenes are highly versatile compounds: biologically they are light-harvesting antennas and are responsible for triggering the vision signal. Long polyenic chains appear also in vitamins and antibiotics. The polymeric form, namely polyacetylene, is naturally photoconductive and becomes conductive upon doping, with conductivities that rival that of copper. Polyenes are also a formidable checkpoint for quantum chemical theory because they are the first class of molecules for which the description of the lowest excited state requires the inclusion of configurations with two excited electrons. This together with the occurrence of phenomena such as sudden polarization effect in the vision process, and the double bond stretch frequency increase upon electronic excitation, makes polyenes an intriguing subject of investigation.

To understand their biological role and to extend their range of application, it is essential to possess a detailed knowledge of the potential energy surfaces of the ground and electronically excited states, together with information on the interstate vibroelectronic and spin–orbit couplings. To this end a large amount of experimental and theoretical data is being gathered. Two authoritative reviews[1] have discussed the advances in this area in earlier stages. The aim of this contribution is to review the experimental and theoretical headway that has been made in this area since the last review was written almost a decade ago.[1] The main emphasis is with the short polyenes (butadiene, hexatriene, and octatetraene), but some aspects of larger polyenes are also considered. Ethylene, which is the basic unit on which polyenes are built, although itself not a polyene, is also discussed. The important developments in the area of polyacetylene and of polyene derivatives of biological interests are not considered in this paper since they have been the object of several authoritative reviews.[2,3]

In this review we start with a brief discussion of two issues that remained partly unresolved at the time the review[1] was written: namely, the ground-state structure of long polyenes and the electronic-state ordering of short ones. Then, we discuss the ground-state vibrational force field and introduce a model to explain the frequency increase of the double bond C=C stretch vibration upon excitation to the $2A_g$ state. We also review the state of experiment and theory of the lowest singlet and triplet states of polyenes. Finally, we close with a look at their photophysical properties.

2. Ground-State Structure of Long Polyenes

At the time when the previous long review[1] on polyenes was written, there was still some debate on the structure of long polyenes. In this respect, two issues must be addressed: (1) bond alternation in long polyenes and (2) planarity of s-cis conformers.

† Università di Bologna.
‡ National Research Council of Canada.

0009-2665/91/0791-0867$09.50/0

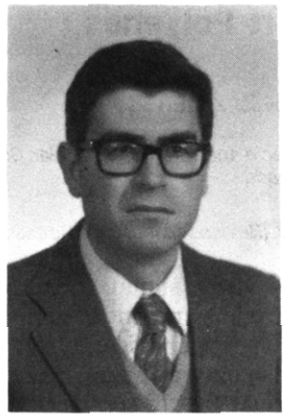

Giorgio Orlandi was born in Verona (Italy) in 1941 and received his degree in Chemistry from the University of Padua in 1964. Following a postdoctoral year with W. Siebrand (National Research Council of Canada, Ottawa, Canada), he joined the National Research Council of Italy. In 1981, he moved to the University of Bologna where he is Professor of Physical Chemistry. His current research deals mainly with the theoretical analysis of spectroscopic and photophysical properties of polyenes, diarylpolyenes, and aromatic systems.

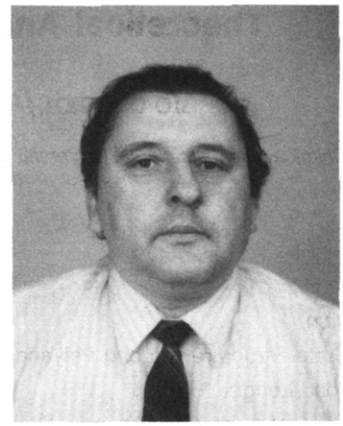

Marek Z. Zgierski was born in Poland in 1946. He received his Ph.D. in 1971 and D.Sc. in 1976 from the Jagiellonian University in Cracow, Poland, where he worked as a research assistant and an adjunct in 1967–1977. In 1977 he joined National Research Council of Canada in Ottawa, Canada, where he presently is a Senior Research Officer. His scientific interests include theory of vibronic coupling with applications to electronic and resonance Raman spectroscopy of polyatomic molecules, radiationless transitions, optical activity, and large amplitude vibrations in the ground and excited states of molecules.

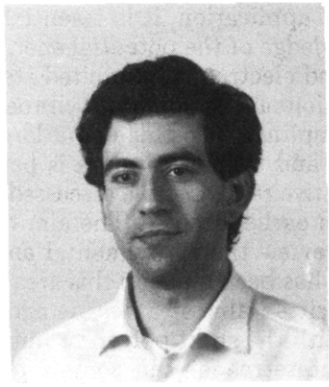

Francesco Zerbetto was born in Milan, Italy, in 1959. He graduated from the University of Bologna in 1982 and received his Doctorate in 1986. He was Research Associate at the National Research Council of Canada, Ottawa, Canada (1986–1990). His research interests include vibrational and electronic spectroscopy, quantum mechanical tunneling, and Monte Carlo simulations.

2.1. CC Bond Length

The structure of the shortest polyenes was determined by electron diffraction for butadiene and hexatriene[4,5] and by X-ray diffraction for octatetraene.[6] Single and double bonds were found to be 1.45 and 1.34 Å, respectively. The bond alternation was confirmed by theoretical calculations.[7-9]

The theory of Peierls instability[10] indicates that even in the infinite-chain limit, bond alternation should occur. Salem[11] has discussed at some length the experimental and quantum mechanical arguments that lead to this conclusion. However, the intuitive notion that for infinitely long polyenes the distinction between single and double bonds vanishes is also appealing. It has been suggested[1,12] that a chain-length increase might decrease the length of the single bonds and increase the length of the central double bond.

The extent of bond alternation in long polyenes is central to the understanding of electronic interactions in π-electron systems: in fact, the one-electron resonance interaction term (which is the only one retained in Hückel-type Hamiltonians) tends to delocalize the π-electrons over the whole carbon skeleton and to make all the CC bonds equivalent. On the other hand, Coulomb repulsion localizes the electrons at different electronic sites and favors alternating CC bond lengths. The balance between these two terms determines the nature of the ground-state structure of polyenes.

To establish which geometry prevails in long polyenes, quantum chemical calculations at different levels of theory have been performed. Hartree–Fock calculations for C_nH_{n+2} with n up to 22, which employed the 6-31G** basis set, yield central C=C and C—C bond lengths of 1.338 and 1.450 Å,[13] respectively. These geometries are in good agreement with the structure obtained with the MNDO method[14] by Boudreaux et al.[15] QCFF/PI[16,17] semiempirical calculations for n up to 36 yield 1.344 and 1.463 Å CC bond lengths.[18] These values are to be compared with experimental results of 1.360 and 1.440 Å, respectively.[19,20] Thus, it is now accepted that, even for infinite polyenes, CC bond alternation does exist, the difference between long and short bonds being about 0.08 Å.

2.2. Structure of s-Cis Conformers: The Butadiene Case

Polyenes can rotate about "single" bonds very easily. At room temperature, the population distribution of different conformers follows Boltzmann's law. Generally, s-trans conformers are more stable because they minimize steric interactions. The same interactions tend to distort s-cis conformers away from planarity. The question of whether the metastable conformer of butadiene is a planar s-cis structure or a gauche structure has been extensively studied. Experimentally observed hot bands and overtones of the Raman spectrum of butadiene that belong to the single bond torsional mode were analyzed to obtain structural information. Unfortunately, the portion of the spectrum recorded appears to be compatible with both structures.[21,22] Different analyses based on a single minimum

potential[21] and a double-minimum potential[22] could both account for the observed spectrum. Polarized infrared spectra of the matrix isolated metastable conformer provides strong evidence for a planar s-cis structure.[23,24] On the other hand, all recent quantum chemical calculations[24-30] find the gauche structure, characterized by a torsional angle between 30° and 41°, to be more stable than the planar s-cis form by about 1 kcal/mol. Possible ways to reconcile theoretical results with polarized infrared spectra have been discussed by Michl and co-workers.[24]

3. Electronic States

In this section, we discuss the energy of the lowest excited states of singlet and triplet spin multiplicity. As is well-known, the two lowest excited states in polyenes are the 1^1B_u state of HOMO → LUMO parentage, to which the transition from the ground state is dipole allowed, and the 2^1A_g state, which is dipole forbidden in the usual one-photon transitions. The 2^1A_g state in polyenes and diphenylpolyenes was first observed by Hudson and Kohler[31,32] as a nearly forbidden transition below that to the 1^1B_u state in the spectrum of α,ω-diphenyloctatetraene. Karplus and Schulten showed this state to be of A_g symmetry[33] by using the semiempirical Pariser–Parr–Pople (PPP) hamiltonian. Simple MO theory fails to describe this state properly and yields energies that are too high. However a simple description can be obtained in VB theory[34] since this state corresponds to a typical VB excitation.[33,35] To account properly for the character of the $2A_g$ state (hereafter we omit the spin index for singlet states) in MO theory, configuration interaction with doubly excited configurations must be used,[33,35-37] since this state is a mixture of singly and doubly excited configurations. The former correspond to $|\text{HOMO}-1\rangle \rightarrow |\text{LUMO}\rangle$ and $|\text{HOMO}\rangle \rightarrow |\text{LUMO}+1\rangle$ excitations whereas, among the latter, the most important is the $|\text{HOMO,HOMO}\rangle \rightarrow |\text{LUMO,LUMO}\rangle$ excitation. The calculated energy of the $2A_g$ state is very sensitive to the chosen geometry of the molecule. Thus the proper energy of this state is obtained only at its optimized geometry. Semiempirical calculations for the ground-state geometry may yield an energy for this state that is higher than that of the $1B_u$ state. However such calculations yield the energy of a vertical excitation from the ground state, i.e., the Franck–Condon maximum, rather than the energy of the electronic origin.

Ab initio calculations indicate that the conformation of the $2A_g$ state in the shortest two polyenes, butadiene and hexatriene, differs from the planar configuration[38,39] at variance with what is observed in longer polyenes.[39] The nonplanar geometry in the $2A_g$ state leads to a vibrational structure associated to torsional modes in the $1A_g \leftrightarrow 2A_g$ transition and is thought to be responsible for the vanishing fluorescence quantum yield in these two molecules.[38] The out-of-plane twisting reflects the balance between two effects: the tendency of an isolated double bond to assume a perpendicular configuration upon excitation, as in ethylene, and the tendency to keep all conjugated double bonds in the same plane so as to allow full electron delocalization.

The $2A_g$-below-$1B_u$ energy ordering is well-documented[40-49] for molecules embedded in matrices at low temperature and appears to be a general characteristic of all polyenic systems.[32] Direct observation of the electric-dipole forbidden $1A_g \rightarrow 2A_g$ transition was achieved by two-photon spectroscopy.[40,49-52] The $2A_g$ state has been detected in absorption or excitation spectra, predominantly in matrices at low temperature; on the other hand, the $1B_u$ state has been observed both in the condensed phase[42-45] and in supersonic beams.[46,53,54] A list of 0–0 excitation energies to the $1B_u$ and $2A_g$ states is given in Table 1. Notice that the energy of the $1B_u$ state depends on the matrix and is usually 3000 cm^{-1} lower in the matrix than in the gas phase. The energy of the $2A_g$ state is much less sensitive to the matrix environment; a discussion of the different behavior of the two states is given by Hudson and Kohler.[1,32] Both theory and experiment agree that the energy gap between the $1B_u$ and $2A_g$ states[1] increases with increasing chain length.

TABLE 1. 2^1A_g–1^1A_g and 1^1B_u–1^1A_g Transition Energies (cm^{-1}) of Polyenes

compound	2^1A_g	1^1B_u
butadiene	(45 000)[a]	46 260,[b] 43 900[c]
hexatriene	34 038[d]	39 783,[b] 36 850[c]
octatetraene	28 560,[e] 28 670[f]	35 550,[g] 32 280,[c] 35 523[h]
decapentaene	24 440[i]	29 030,[c] 29 600[i]
dodecahexaene		27 536[j]
2,12-dimethyl-tridecahexaene	21 750[k]	25 750[k]
hexadecaheptaene	19 522[l]	24 178[l]
hexadecaoctaene	17 871[m]	22 770[m]

[a] Reference 58, in gas phase. [b] Reference 53, in supersonic beams. [c] Reference 45, in matrix at 77 K. [d] Reference 59, in collision-free beam. [e] Reference 40, in matrix at 4 K, one- and two-photon excitation. [f] Reference 46, in matrix at 77 K. [g] Reference 54, in supersonic beam. [h] Reference 46, in gas phase. [i] R. L. Christensen, quoted in ref 37 in matrix. [j] Reference 45, in matrix at 293 K. [k] Reference 47, in matrix at 4 K. [l] Reference 43, in matrix at 10 K. [m] Reference 44, in matrix at 4.2 K.

For a long time, butadiene and hexatriene, which are nonfluorescent, were thought to be exceptions to the rule that the $2A_g$ state of polyenes lies below the $1B_u$ state, because the transition to the $2A_g$ state could not be located either in absorption or in energy-loss spectra.[55-57] Only indirect evidence, provided by resonance Raman spectra in the gas phase, was available for the location of the $2A_g$ state in butadiene:[58] the weak activity of the b_u mode of frequency ν_{24} = 300 cm^{-1}, noted only in the excitation interval 5.4–5.8 eV, suggested that the $2A_g$ state is located around 5.6 eV. However, very recently, through multiphoton ionization in a collision free beam, direct observation of the $2A_g$ state was achieved for *cis*- and *trans*-hexatriene.[59] This state was found to be 5270 and 5748 cm^{-1} below the $1B_u$ for *cis*- and *trans*-hexatriene, respectively. Given this large energy gap, it is highly likely that also in butadiene the $2A_g$ state lies below the $1B_u$ state, in agreement with the suggestion of Chadwick et al.[58] The determination of the correct ordering of the two lowest excited singlet states of ab initio methods is a difficult task and one that requires very extensive calculations. This is due to the difficulty of treating in a balanced way the $2A_g$ and $1B_u$ states, since they are of different nature being of covalent and ionic type, respectively. Thus the use of a standard basis set (like a DZ basis set) and of a CI treatment restricted to the $\pi\pi^*$ space leads to a more realistic description of the $2A_g$ state than of the $1B_u$ state. Very accurate calculations to determine the ordering of these states in butadiene,[60,61] hexatriene,[61,62]

TABLE 2. 0–0 and Vertical Calculated and Observed Transition Energies (eV) of the 2^1A_g, 1^1B_u, and 1^3B_u Electronic States (Vertical Energies in Parentheses)

	2^1A_g		1^1B_u		1^3B_u	
compound	expt	theory	expt	theory	expt	theory
butadiene	5.40[a]	5.66 (6.67)[b]	5.73[c]	5.74 (6.23)[b]	2.59[d]	(–)
hexatriene	4.22[e]	4.52 (5.74)[f]	4.93[c]	4.68 (5.14)[b]	2.03[g] (2.7)[h]	(2.8)[f]
octatetraene	3.59[i]	4.15 (5.21)[j]	4.41[k]	4.56 (4.79)[j]	1.70 (2.20)[l]	(2.5)[j]

[a] Reference 58. [b] References 60, 61. [c] Reference 53. [d] Reference 69. [e] Reference 59. [f] References 61, 62. [g] Reference 70. [h] Reference 57. [i] Reference 40. [j] Reference 63. [k] Reference 54. [l] Reference 71.

and octatetraene[63] have been recently performed by Davidson and co-workers. These calculations employed TZ (butadiene) and DZ (hexatriene and octatetraene) basis sets, augmented with polarization and diffuse functions. To obtain reliable results, extensive configuration interaction in the $\sigma\pi^*$ space was required. The structures used in the calculations were both the ground-state equilibrium geometry and the optimized geometries of the $1B_u$ and $2A_g$ states taken from ref 7. The excitation energies for the vertical and 0–0 transitions calculated in this way are shown in Table 2. In agreement with the experimental results, they find the $2A_g$ state to be the lowest in the three molecules considered. It appears that although for the ground state geometry the $1B_u$ state lies below the $2A_g$ state, the 0–0 transition occurs at lower energies for the $2A_g$ state than for the $1B_u$ state. These results should also serve as a warning against the use of single-point calculations to assess the energy ordering of electronically excited states. Other recent ab initio calculations on the lowest singlet states of short polyenes are reported in refs 38 and 64–68. In Table 2 are also shown the energies of the lowest triplet state, 1^3B_u, of hexatriene and octatetraene obtained at the S_0 geometry by the same ab initio calculations employed for the singlet states.[61-63] These energies calculated for the 1^3B_u state compare well with available experimental data.[69-75]

There is an aspect of recent semiempirical CI calculations[36] that seems to have been so far overlooked by the experimental investigators in this field. Tavan and Schulten predicted that starting from dodecahexaene, the weak vertical transition to the $1B_u^-$ state occurs at energies lower than that to the strongly allowed $1B_u^+$. In particular, they predicted an energy gap decreasing with chain length between the $1B_u^-$ and the $2A_g^-$ state. Although spectra of long polyenes are available, to the best of our knowledge, no attempt has been made to locate this transition. The position of this state is significant for resonance Raman scattering spectra, for the vibrational structure of the $1A_g \rightarrow 2A_g$ transition, and for the photophysics of long polyenes.

4. Ground-State Vibrations

The vibrational frequencies of *all-trans*-butadiene, -hexatriene, and -octatetraene together with *s-cis*-butadiene and *cis*-hexatriene have been thoroughly investigated. For longer polyenes, from decapentaene to hexadecaoctaene, we have only a limited knowledge of the frequencies of totally symmetric modes obtained from fluorescence spectra. The identification and assignment of normal-mode frequencies can now be achieved with great confidence due to the possibility of calculating reliable force fields.

Before reviewing results for individual molecules, we discuss briefly the theoretical methods that have proved most useful in analyzing vibrational spectra of polyenes. They can be loosely divided into three groups: semiempirical, ab initio, and ab initio followed by empirical scaling of the force constants. The semiempirical methods that are popular to calculate vibrational frequencies are MNDO[14] and its AM1[76] parametrization and the QCFF/PI model;[16,17] the former are Hamiltonians wherein all the valence electrons are treated explicitly, the latter describes the σ-electrons through an empirical potential and the π-electrons through a modified PPP Hamiltonian and includes configuration interaction. The QCFF/PI model produces accurate force fields,[77-79] especially for polyenes,[7,80-90] and has the advantage of being applicable to fairly large systems which are not within reach of other theoretical methods. Since semiempirical methods rely on parameters derived from experimental data of few prototype molecules, they are very economic but may be inaccurate. For example, an incorrect assignment of experimental frequencies can lead to systematic errors in the calculated frequencies.

The second approach is based on straightforward ab initio MO calculations. To obtain reliable results, large basis sets and an adequate treatment of electron correlation are required. Electron correlation is usually introduced directly via CI, by adding the perturbative Møller–Plesset (MP) correction[91] to SCF results, or, alternatively, by performing multiconfiguration self-consistent field (MCSCF)[92,93] calculations. With the last approach it is possible to obtain reasonably accurate, although somewhat overestimated, vibrational frequencies. Recent calculations of the vibrational force field of *s-cis*-butadiene are a typical example.[24-26] The advantage of this highly CPU-intensive method is that it is completely unbiased, since it does not make any arbitrary assumption, so that it is perfectly equipped to correct possible misassignments of vibrational frequencies.

The third approach is also based on ab initio calculations. Basis set deficiencies and neglect of electron correlation are compensated through suitable scaling of the calculated force field. It has been shown that scale factors are transferable within the same class of molecules;[94-97] the most popular scaling procedure is the SQM (scaled quantum mechanical) method introduced by Pulay.[97] This approach can deal with fairly large systems; however, due to the partly empirical corrections used in the treatment, it may run into difficulties when electron correlation affects a specific normal mode (vide infra).

All of these approaches have been applied to the study of vibrations in polyenes and have yielded very similar results. We now proceed to discuss the force fields and the vibrational assignment of shorter polyenes.

TABLE 3. Observed and Computed Vibrational Frequencies (cm^{-1}) of Butadiene in the S_0 State (CH Stretches Are Omitted)

symmetry	experiment	theory	description
a_g	1644[a] 1643[b]	1665[c] 1656[d] 1631[e]	CC
	1441[a] 1442[b]	1458[c] 1447[d] 1451[e]	CH_2 sciss
	1279[a] 1291[b]	1299[c] 1291[d] 1303[e]	CH rock
	1206[a] 1205[b]	1215[c] 1214[d] 1208[e]	CC
	887[a] 890[b]	882[c] 880[d] 872[e]	CH_2 rock, CC
	513[a] 513[b]	502[c] 515[d] 532[e]	CCC bend
b_u	1597[a] 1599[b]	1596[c] 1591[d] 1593[e]	CC
	1381[a] 1385[b]	1398[c] 1380[d] 1395[e]	CH_2 sciss
	1297[a] 1296[b]	1302[c] 1303[d] 1289[e]	CH rock
	988[a] 991[b]	999[c] 993[d] 981[e]	CH_2 rock
	301[a] 301[b]	287[c] 289[d] 343[e]	CCC bend
a_u	1022[a] 1013[b]	1017[c] –[d] 1055[e]	CH wag
	905[a] 908[b]	913[c] –[d] 948[e]	CH_2 wag
	535[a] 524[b]	516[c] –[d] 534[e]	C=C tors
	163[a] 163[b]	163[c] –[d] 180[e]	C–C tors
b_g	974[a] 967[b]	968[c] –[d] 978[e]	CH wag
	908[a] 911[b]	913[c] –[d] 946[e]	CH_2 wag
	754[a] 753[b]	749[c] –[d] 661[e]	C=C tors

[a] Reference 101, infrared and Raman spectra in low temperature matrices. [b] Reference 100. [c] Reference 97, 4-21G SCF calculation followed by scaling. [d] Reference 8, TZP CPF calculation followed by scaling. [e] Reference 84, QCFF calculation including CI-SD.

TABLE 4. Observed and Computed Vibrational Frequencies (cm^{-1}) of Butadiene-d_4 and Butadiene-d_6 in the S_0 State (CH Stretches Omitted)

	butadiene-d_4		butadiene-d_6	
symmetry	expt[a]	theory[b]	expt[a]	theory[b]
a_g	1612	1602	1592	1570
	1040	1035	1050	1057
	1298	1300	925	895
	1170	1211	1199	1240
	740	713	743	713
	454	471	445	460
b_u	1533	1530	1511	1518
	1028	1017	1043	1054
	1274	1283	989	985
	811	811	738	742
	258	294	250	286
a_u	968	989	766	794
	722	757	715	740
	404	404	391	391
	149	165	142	156
b_g	940	910	800	787
	728	756	705	702
	620	550	603	550

[a] Reference 101, infrared and Raman spectra in low temperature matrices. [b] Reference 84, see Table 3.

4.1. *all-trans*-Polyenes

all-trans-Polyenes belong to the C_{2h} point group and their normal coordinates transform as the a_g, b_u, a_u, and b_g irreducible representation; a_g and b_u are in plane modes, while a_u and b_g are out of plane vibrations.

4.1.1. Butadiene

In butadiene there are nine a_g, eight b_u, four a_u, and three b_g modes. All the vibrational frequencies have been observed in IR or Raman spectra,[1,98-101] and the corresponding force field has been obtained by several theoretical calculations.[8,39,64,84,97,102-104] A list of observed and calculated frequencies is given in Table 3. The agreement between calculated and observed frequencies is quite good. The vibrational assignment has been confirmed through the study of the isotopic shifts in five isotopomers.[100,101,105-107] The calculated and observed frequencies of butadiene-d_4 and -d_6 are shown in Table 4. Also the vibrational spectra of methylated butadienes have been observed and assigned.[90,108-110] Notice the systematic underestimation of the frequency of the b_g C=CH_2 torsional vibration by the QCFF/PI method (661 vs 754 cm^{-1} in butadiene, 550 vs 620 cm^{-1} in butadiene-d_4, and 550 vs 603 cm^{-1} in butadiene-d_6). These discrepancies result from the experimental assignment of this frequency as 680 cm^{-1} (later revised to 754 cm^{-1}) at the time in which the QCFF/PI parameterization was proposed.[16]

TABLE 5. Observed and Computed Vibrational Frequencies (cm^{-1}) of *trans*-Hexatriene in the S_0 State (CH Stretches Are Omitted)

symmetry	expt[a]	theory[b]	description
a_g	1623	1662 (1619)	CC
	1574	1583 (1577)	CC
	1397	1414 (1414)	CH_2 sciss
	1320[c]	1313 (1350)	CH rock
	1288	1288 (1294)	CH rock
	1188	1198 (1192)	CC
	930	926 (931)	CH_2 rock
	444	432 (457)	CCC bend
	353	340 (385)	CCC bend
b_u	1629	1634 (1618)	CC
	1433	1445 (1443)	CH_2 sciss
	1296	1301 (1302)	CH rock
	1255	1270 (1271)	CH rock
	1132	1126 (1179)	CC
	966	957 (944)	CH_2 rock
	541	530 (578)	CCC bend
	152	143 (175)	CCC bend
a_u	1008	1026 (1057)	CH wag, C=CH_2 tors
	938	953 (960)	CH wag
	900	922 (943)	CH_2 wag
	683	679 (621)	C=CH_2 tors, CH wag
	248	242 (242)	C=C tors
	94	94 (106)	C–C tors
b_g	985	1000 (1022)	CH wag, C=CH_2 tors
	901	929 (948)	CH_2 wag
	868	874 (823)	CH wag
	478	590 (596)	C=CH_2 tors, CH wag
	215	211 (228)	C–C tors

[a] Reference 114. [b] Reference 115, in parentheses from ref 84. [c] Reference 113.

4.1.2. Hexatriene

There are 13 a_g, 12 b_u, 6 a_u, and 5 b_g modes in hexatriene. All the vibrational frequencies have been observed by several authors;[111-114] Langkilde et al.,[114] who reinvestigated the vibrational assignment of this molecule, have reviewed most of the previous work. The few discrepancies left between the two most recent assignments[113,114] have been resolved by quantum chemical evaluation of the force field.[7,8,87,107,115,116] A list of calculated and observed frequencies is given in Table 5. The major difference between experimental and theoretically aided assignment concerns ν_{23}, a b_g C=C torsion, which is empirically assigned to the 428 cm^{-1} band, whereas calculations, both ab initio and semiempirical, yield about 600 cm^{-1}. In our view, this difference is large enough to suggest a revision of the empirical assignment. Many of the vibrational assignments have been confirmed by the study of deuterated isotopomers.[89,112,117]

4.1.3. Octatetraene

There are 17 a_g, 16 b_u, 8 a_u, and 7 b_g modes in octatetraene. Most of the frequencies have been reported

TABLE 6. Observed and Computed Vibrationl Frequencies (cm^{-1}) of *trans,trans*-Octatetraene in the S_0 State (CH Stretchs Are Omitted)

symmetry	expt[a]	theory[b]	description
a_g	1613	1617 (1614)	CC
	1608[c]	1614 (1600)	CH
	1423	1441 (1439)	CH_2 sciss
	1299	1316 (1366)	CH rock
	1291	1304 (1313)	CH rock
	1281	1288 (1290)	CH rock
	1179	1187 (1188)	CC
	1136	1124 (1181)	CC
	956	954 (950)	CH_2 rock
	538	528 (583)	CCC bend
	343	334 (337)	CCC bend
	242[c]	215 (257)	CCC bend
b_u	1632	1634 (1622)	CC
	1558–1569	1584 (1567)	CC
	1405	1423 (1422)	CH_2 sciss
	1303	1317 (1334)	CH rock
	1280	1293 (1297)	CH rock
	1229	1245 (1248)	CH rock
	1139	1138 (1187)	CC
	940[d]	929 (930)	CH_2 rock
	565	559 (594)	CCC bend
	390	377 (439)	CCC bend
	96	84 (104)	CCC bend
a_u	1011	1027 (1059)	CH wag
	960	976 (996)	CH wag
	900	926 (947)	CH_2 wag
	840	843 (814)	CH wag
	629	617 (608)	C=CH_2 tors
	245	239 (254)	C–C tors
	181	167 (170)	C=C tors
		58 (66)	C–C tors
b_g	1080[c]	1011 (1039)	CH wag
	958[c]	943 (954)	CH wag
	896	923 (942)	CH_2 wag
	877	892 (842)	CH wag
	722[c]	654 (611)	C=CH_2 tors
	343	336 (321)	C=C tors
	164[c]	146 (159)	C–C tors[d]

[a] Reference 118. [b] Reference 9, in parentheses from ref 84. [c] Reference 1. [d] Reference 119.

TABLE 7. Observed and Computed Vibrational Frequencies (cm^{-1}) of *s-cis*-Butadiene in the S_0 State (CH Stretches Are Omitted)

symmetry	expt[a]	theory[a]	description
a_1	1612[b]	1706	CC
	1425	1515	CH_2 sciss
		1392	CH rock
		1097	CH_2 rock
		907	CC
	596	309	CCC bend
a_2	984	1018	CH wag
	920	907	CH_2 wag
	730	739	C=C tors
	136[c]	165i	C–C tors
b_1	1633	1721	CC
	1403	1480	CH_2 sciss
		1343	CH rock
	1087	1136	CH_2 rock
	530	570	CCC bend
b_2	996	1041	CH wag
	914	921	CH_2 wag
	470	520	C=C tors

[a] Reference 24. [b] Reference 121. [c] Reference 101.

by Yoshida and Tasumi[118] and by Lippincott and coworkers.[119] Further information was also provided by Kohler and Snow[120] and by unpublished spectra by Holtom, McClain, and Kohler referenced in Table VII of ref 1. Theoretical calculations[9,84] have been very

TABLE 8. Observed and Computed Vibrational Frequencies (cm^{-1}) of *cis*-Hexatriene in the S_0 State (CH Stretches are Omitted)

symmetry	expt[a]	theory[b]	description
a_1	1623	1674 (1619)	CC
	1578	1569 (1565)	CC
	1397	1412 (1423)	CH_2 sciss
	1315	1324 (1325)	CH rock
	1246	1278 (1241)	CH rock, CC
	1082	1088 (1118)	CC, CH rock
	884	868 (884)	CH_2 rock
	394	385 (417)	CCC bend
	170	164 (201)	CCC bend
b_1	1623, 1612[c]	1633 (1615)	CC
	1452	1463 (1468)	CH_2 sciss
	1395[c]	1371 (1397)	CH rock
	1278	1291 (1297)	CH rock
	1187	1195 (1217)	CC
	954	948 (937)	CH_2 rock
	680	677 (705)	CCC bend
	353	347 (410)	CCC bend
a_2	1032, 990[c]	1010 (1049)	CH wag
	952	962 (961)	CH wag
	907	909 (943)	CH_2 wag
	707	702 (649)	C=CH_2 tors
	332	327 (350)	C=C tors
	155	143 (168)	C–C tors
b_2	989	996 (1017)	CH wag
	906	916 (948)	CH_2 wag
	815	781 (764)	CH wag
	585	573 (597)	C=CH_2 tors
	100	96 (113)	C=C tors

[a] Reference 114. [b] References 116, in parentheses ref 84. [c] Reference 113.

TABLE 9. Force Constants *K* (mdyn/Å) for the CC Stretches in the S_0 State of *trans*- and *cis*-Polyenes

	SQM[a]		SQM[b]		PPP-CI[c]	
bond	trans	cis	trans	cis	trans	cis
C_i=C_{i+1}	8.04	8.04	8.43	8.43	8.30	8.30
C_i–C_{i+1}	4.96	4.88	5.08	4.97	5.63	5.70
C_i=C_{i+1}, C_{i+1}—C_{i+2}	0.31	0.32	0.51	0.54	0.72	0.80
C_i=C_{i+1}, C_{i+2}=C_{i+3}	–0.08	–0.09	–0.19	–0.21	–0.14	–0.14
C_i–C_{i+1}, C_{i+2}–C_{i+3}	–0.05	0.02	–0.09	–0.04	–0.05	0.02
C_i=C_{i+1}, C_{i+3}—C_{i+4}	0.03	0.02	0.07	0.05	0.03	0.03

[a] Reference 116, ab initio, 6-31G basis set, SQM force field. [b] Reference 9, ab initio, 4-21G basis set, SQM with special scaling factors for off-diagonal CC force constants. [c] Reference 84.

TABLE 10. Experimental (Calculated) $1A_g$ and $2A_g$ State C=C Stretch Frequencies (cm^{-1}) for Some Conjugated Compounds

compound	$1A_g$	$2A_g$
2,10-dimethylundecapentaene[a]	1598 (1575)	1737 (1710)
octatetraene[b]	1608 (1601)	1754 (1711)
2,12-dimethyltridecahexaene[c]	1576 (1565)	1779 (1722)
diphenyloctatetraene[d]	1580 (–)	1680 (–)
N-dodecapentaenylidenebutylamine[e]	1589 (1624)	1544 (1676)
dodecapentaenal[f]	1575 (1619)	1636 (1603)
hexadecaheptaene[g]	1555 (1552)	1782 (1716)
hexadecaoctaene[h]	1555 (1550)	1779 (1708)
β-carotene[i]	1521 (–)	1777 (–)

[a] Reference 41. [b] Reference 40. [c] Reference 42. [d] Reference 125. [e] Reference 47. [f] Reference 126. [g] Reference 43. [h] Reference 44. [i] Reference 127.

helpful in the assignment of experimental frequencies. A list of experimental frequencies selected to match the theoretical results is given in Table 6. In our opinion, there is some uncertainty in the assignment of the b_g C=CH_2 torsional frequency, given the sizeable difference between the value of this frequency calculated ab

initio (654 cm^{-1}) and that assigned experimentally (722 cm^{-1}).

4.2. *cis*-Polyenes

4.2.1. s-cis-Butadiene

Spectroscopically, *s-cis*-butadiene has been studied quite thoroughly.[23,24,106,121] However, some vibrational frequencies are as yet not assigned or are controversial. Experimental and calculated frequencies are reported in Table 7, where Michl and co-workers assignment is followed.[24] This assignment is based on polarized IR spectra which indicate that the molecular symmetry is C_{2v}. Whether the metastable conformer of butadiene is s-cis or gauche (vide supra) is still controversial. All but one of the assignments given in Table 7 are supported by ab initio calculations,[24-28] the only exception being the totally symmetric CCC bend which is calculated to be about 300 cm^{-1} and is empirically assigned to the 596 cm^{-1} band. This is a strikingly large difference, suggesting that the empirical assignment ought to be revised. Obviously, the a_2 C–C torsion is calculated to have an imaginary frequency at the s-cis conformation. By inspection, a number of differences emerge between the s-trans and the s-cis normal modes and frequencies: the CH_2 rocks have a higher frequency in the s-cis conformer, the C–C stretch frequency is much higher in s-trans (1205 cm^{-1}) than in s-cis (900 cm^{-1}). The C=C stretch frequencies are more split for s-trans than for s-cis; also the antisymmetric stretch has a higher frequency than the symmetric stretch in the cis conformer, while this ordering is reversed in the trans conformer. A similar frequency inversion is observed for the CCC bends. An analysis of the **G** and **F** matrices shows that these inversions are caused mainly by the former.

4.2.2. cis-Hexatriene

The vibrational frequencies of *cis*-hexatriene have been extensively studied. Vibrational spectra were recorded by several authors[112-114,122,123] and all the bands are assigned (see Table 8). Quantum chemical calculations[84,89,103,116,123] and the study of deuterated and methylated derivatives support the assignments.[116,124] By comparing *cis*- and *trans*-hexatriene frequencies, we notice a 100 cm^{-1} difference between the two C–C totally symmetric frequencies (1082 vs 1188 cm^{-1}). Also some symmetry inversions similar to those in butadiene are noticed.

4.3. Ground-State Force Field of Polyenes

Vibrational properties are usually best understood in terms of force field constants. Average values of CC stretch force constants for *cis*- and *trans*-polyenes calculated by three different methods are given in Table 9. The differences between *cis*- and *trans*-polyene force constants are rather small and cannot cause large frequency shifts upon cis–trans isomerization. These shifts are mainly due to changes in the **G** matrix. Since steric interactions greatly affect CCC bond angles, fairly large changes are expected in the **G** matrix. Indeed, off-diagonal elements between adjacent CCC bends change sign upon isomerization about the common CC bond. To second order, this entails a change of coupling between second nearest CC bonds, contributing to changes in the CC stretch frequencies upon isomerization.

Comparison of force constants calculated with three different methods shows that the most prominent difference occurs for the off-diagonal force constant between two adjacent CC bonds. This force constant goes from 0.3 mdyn/Å, obtained by the ab initio SCF-MO SQM method, to 0.7 mdyn/Å, found by the PPP-CI method.[90] In terms of vibrational frequencies, the SCF-MO SQM overestimates the Franck–Condon-active CC stretch frequency, whereas the PPP-CI method slightly underestimates it. It was found[8] that adding electron correlation to the SCF wave function increases the off-diagonal element and decreases the CC-stretch frequency. Pulay et al.[9] found that the optimum value for this constant lies in the 0.50–0.54 mdyn/Å range, i.e. closer to the PPP-CI calculations. It appears (vide infra) that most of the correlation contribution to this C=C stretch off-diagonal force constant is related to the dependence of the S_0–S_1 interaction on the displacement along the Franck–Condon-active CC stretch, which is a linear combination of local CC stretches with alternate signs.

5. Vibronic Coupling in Polyenes

5.1. Frequency Increase upon $S_0 \rightarrow S_1$ Excitation

As we have seen in the preceding section, the ground-state frequency of the Franck–Condon-active C=C stretch is described correctly only by quantum mechanical treatments including electron correlation. The frequency of this mode shows a quite peculiar property; namely, it is observed to increase upon excitation to the $2A_g$ state. In Table 10, we show a number of these increases. Similar unconventional behavior is exhibited by the ν_{14} mode of the b_{2u} symmetry in benzene[128,129] and by the ν_{21} mode of the b_{2u} symmetry in naphthalene.[130] At first, the frequency increase of the Franck–Condon-active CC stretch mode upon $1A_g \rightarrow 2A_g$ excitation seemed puzzling, since the electron density in the double bonds is expected to decrease upon excitation, causing a decrease in bond order and hence in vibrational frequency. It appears that the frequency increase of the C=C stretch mode in the S_1 state and the accompanying anomalously low value of the ground-state frequency of the same mode can be explained in terms of electron correlation; specifically, it can be attributed to the dependence of the S_0–S_1 CI mixing on the geometry.

In order to gain a better understanding of the way these effects arise, we consider two electronic states $|\phi_i\rangle$ and $|\phi_j\rangle$, together with a totally symmetric mode with the coordinate Q, as in the case of polyenes. We assume these states to be eigenstates of the electronic Hamiltonian H at the reference geometry $Q = 0$ only. Thus, these states belong to the class of diabatic states that have been introduced long ago.[131-133] Such states have been applied in several areas of chemical physics and most notably in the theoretical analysis of electronic spectra of molecules.[134-136] The diabatic potential energy curves associated with $|\phi_i\rangle$ and $|\phi_j\rangle$, defined as

$$E_k(Q) = \langle\phi_k|H|\phi_k\rangle;\ k = i, j \qquad (1)$$

are given by

$$E_k(Q) = E_k^0 + 0.5\Omega^2Q^2 + B_kQ;\ k = i, j \qquad (2)$$

where E_i^0 and E_j^0 are the energies at the reference geometry, Ω_0 is the vibrational frequency assumed to be the same in both electronic states, and B_i, B_j are the displacement parameters of the potential energy curves. Since the two states are diabatic, they are coupled by a Q-dependent interaction, U_{ij}, which, for simplicity, we make linear

$$U_{ij} = \langle\phi_i|H|\phi_j\rangle = V_{ij}Q \qquad (3)$$

where V_{ij} is the linear vibronic coupling parameter. If the energy gap between the two states $E_{ji}^0 = E_j^0 - E_i^0$ is large compared to $V_{ij}\bar{Q}$ ($\bar{Q}$ is the mean amplitude) and Ω, the Born–Oppenheimer approximation applies and the molecular states can be described in terms of vibrational potentials. Diagonalization of the 2 × 2 electronic energy matrix yields then adiabatic potentials, which can be written in the harmonic approximation as[137]

$$E_k^{ad}(Q) = E_k^0 + 0.5\omega_k^2Q^2 + B_kQ;\ k = i, j \qquad (4)$$

where the adiabatic frequencies ω_i and ω_j are

$$\omega_i = \Omega(1 - 2V_{ij}^2/E_{ji}^0\Omega)^{1/2} \qquad (5)$$

$$\omega_j = \Omega(1 + 2V_{ij}^2/E_{ji}^0\Omega)^{1/2} \qquad (6)$$

The introduction of vibronic coupling in the diabatic picture leads to the result that the adiabatic frequency in the upper state is increased while that in the lower state is decreased with respect to the diabatic frequency. Thus, even if the diabatic frequency Ω of the ground state is higher than that of the excited state, sufficiently strong vibronic coupling between the two states can reverse the ordering of the adiabatic frequencies, producing an effect such as that observed in the S_0 and S_1 states of polyenes. Moreover, if the equilibrium position of Q in the diabatic representation is $Q_{0,k}$, it becomes $Q_{0,k}(\Omega/\omega_k)^2$ in the adiabatic representation. This model is easily generalized to more than two states coupled by mode Q. The interpretation of the frequency increase of the C=C stretch mode in terms of vibronic coupling was first suggested in ref 42. The adiabatic frequencies in the i and j states are then easily found by perturbation theory:[137]

$$\omega_k = \Omega\sum_{l\neq k}(1 + V_{kl}^2/E_{kl}^0);\ k = i, j \qquad (7)$$

Thus, if i and j represent the $1A_g$ and $2A_g$ states of polyenes, respectively, the frequency of the (totally symmetric) mode Q is depressed in the $1A_g$ state by vibronic interactions with all excited electronic states of the proper symmetry. The vibrational frequency of this mode in the $2A_g$ state is, on the other hand, increased by vibronic interaction with the $1A_g$ state, but decreased by interactions with higher nA_g states. It follows that the ground state frequencies are always lowered from their diabatic values by vibronic interactions, while $2A_g$ state frequencies can decrease or increase depending on the relative strength of the $1A_g$–$2A_g$ coupling compared with $2A_g$–nA_g couplings.

To effectively use this model, one has to define the appropriate diabatic electronic wave functions and then calculate, through quantum chemical methods, all the quantities involved, namely E_i^0, Ω, B_i, V_{ij}, ω_i. A convenient choice for the diabatic basis set is provided by MO-CI wave functions that are eigenfunctions of the molecular Hamiltonian H taken at the equilibrium geometry of the ground state and have the MO and CI coefficients fixed, i.e. independent on geometrical parameters. Thus, although electron correlation is taken into account at the reference geometry, its dependence on nuclear coordinates is neglected. Since most of the polyenic systems range well above 10 atoms (actually butadiene itself has already 10 atoms), it is thus unavoidable that a great part of the systematic quantum chemical work has been limited at the semiempirical level of theory. Some excitation energies and ground state adiabatic vibrational frequencies for short polyenes have also been obtained by ab initio calculations (vide supra). Calculations of adiabatic vibronic coupling integrals V_{ij} were performed with the CNDO/S Hamiltonian[138] following the approach of ref 139, which is described in Appendix A. The vibronic coupling constants V_{ij} were calculated for totally symmetric CC stretch vibrations of butadiene, hexatriene, octatetraene, and decapentaene.[137] They are reported in Tables 11 and 12. The largest coupling caused by the Franck–Condon-active mode was found to occur between the $1A_g$ and $2A_g$ states, while the couplings of the

TABLE 11. Vibronic Coupling Integrals V_{ij}[a] (cm^{-1}) between nA_g States Calculated by the CNDO/S Hamiltonian with the Diabatic C=C a_g Modes[b]

	Butadiene				
	$V_{0,1}$	$V_{1,3}$	$V_{1,4}$		
Q_1	2281	1214	1649		
	Hexatriene				
	$V_{0,1}$	$V_{0,5}$	$V_{1,4}$	$V_{1,5}$	$V_{1,7}$
Q_1	2443	1259	785	899	1185
Q_2	459	326	163	1807	726
	Octatetraene				
	$V_{0,1}$	$V_{0,4}$	$V_{0,6}$	$V_{1,4}$	$V_{1,6}$
Q_1	2429	459	1540	326	592
Q_2	415	1436	267	1540	267
	Decapentaene				
	$V_{0,1}$	$V_{0,4}$	$V_{0,7}$	$V_{1,4}$	$V_{1,6}$
Q_1	2295	592	1496	429	503
Q_2	503	1703	489	1170	429
Q_3	-	400	-	770	-

[a] i, j refer to the excited state number, while 0 indicates the ground state. [b] From ref 137.

TABLE 12. Vibronic Coupling Integrals V_{ij}[a] (cm^{-1}) between nB_u States Calculated by the CNDO/S Hamiltonian with the Diabatic C=C a_g Modes[b]

	Butadiene				
	$V_{2,5}$	$V_{2,6}$	$V_{2,8}$		
Q_1	493	398	1029		
	Hexatriene				
	$V_{2,6}$	$V_{2,8}$			
Q_1	154	655			
Q_2	1539	468			
	Octatetraene				
	$V_{2,3}$	$V_{2,7}$	$V_{2,8}$	$V_{2,10}$	
Q_1	67	56	299	927	
Q_2	49	52	1462	545	
	Decapentaene				
	$V_{2,3}$	$V_{2,5}$	$V_{2,8}$	$V_{2,11}$	$V_{2,12}$
Q_1	52	-	36	441	672
Q_2	-	-	179	1352	872
Q_3	-	-	-	89	145

[a] i, j refer to the excited state number. [b] From ref 137.

$2A_g$ and $1B_u$ states with higher states are modest. It follows that not only is the C=C frequency in the S_1 state higher than that in the S_0 state but also the frequency of the same mode in the S_2 state may be higher than that in the S_0 state. The adiabatic frequencies reported in Table 10, calculated from eq 7 with the computed vibronic coupling parameters V_{ij}, reproduce fairly well the frequency increase of the C=C stretch mode upon excitation.[137] Also notice that the larger the ratio between perturbed and unperturbed frequencies, the greater the difference in equilibrium position between the two pictures. This difference is usually small for short polyenes;[134] however, since the coupling V_{01} is constant and the energy gap decreases with the chain length,[86] it can become important for long chains.

Other a_g vibrations which are Franck–Condon inactive were found to be involved in sizeable couplings of the $2A_g$ and $1B_u$ states with higher electronic states although they couple the $1A_g$ state only slightly. These vibrations are associated to "well-behaving" frequencies, namely to frequencies that decrease upon electronic excitation. Vibronic activity of different a_g modes in coupling a given pair of electronic states is responsible for normal mode rotation between different states, i.e. the Dushinsky effect.[141-143] This effect is known to cause changes in vibrational frequencies and in the intensity distribution of electronic spectra. Qualitatively this can be seen if the model is generalized to two vibrational modes. Some details of this effect are given in Appendix B.

The absence of a frequency increase upon excitation in two polyenic derivatives, namely dodecapentaenal and its Schiff base, was considered.[140] It was shown that the $S_0 - S_1$ coupling remains strong, but that a rather small $S_1 - S_2$ coupling, which is symmetry allowed in these derivatives, suffices to reduce the adiabatic frequency to values very similar to the ground state ones.

5.2. Correlation between the C=C Stretch Frequency and the Length of Polyene Chain

This model, explains not only the frequency increase of the Franck–Condon active C=C stretch mode upon $1A_g \rightarrow 2A_g$ electronic excitation, but also the observed correlation between the ground-state frequency of this mode and the position of the maximum of its absorption spectrum, that is the energy of the $1B_u$ state. Since the excitation energy to the $1B_u$ state decreases with the length of the polyene, it follows that the ground-state frequency of the C=C stretch is also correlated with the length of the polyene; the longer the polyene, the lower the C=C stretch frequency.[12] This correlation was first explained by assuming that, with the increase of the polyene length, the π-electron delocalization should tend to equalize CC bond lengths, thus decreasing the bond order of the C=C bonds, resulting in a lower C=C stretch frequency for longer polyenes.[12] However, semiempirical and ab initio quantum chemical calculations indicate that the π-electrons remain relatively highly localized even in very long polyenes resulting in strong CC bond-length alternation.[13,15,18] Indeed, calculations show no systematic changes of C=C and C—C bond lengths with increasing length of the carbon skeleton. On the contrary, starting with octatetraene, the bond lengths remain almost constant and alternate between 1.36 and 1.46 Å,[18] although the

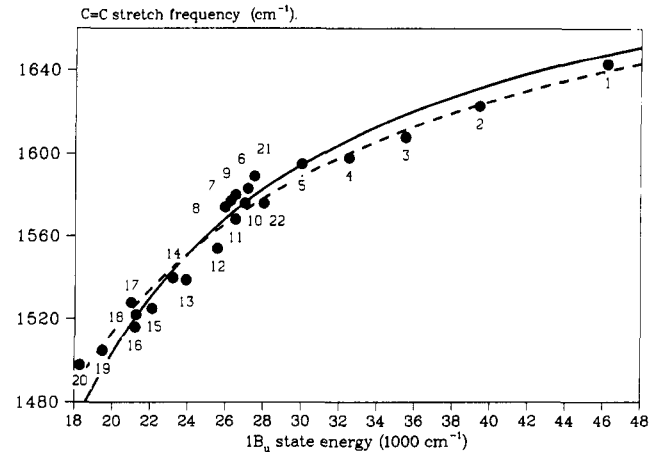

Figure 1. ω(C=C) – E_{1B_u} correlation diagram for various polyenes. Full circles indicate the following molecules: (1) butadiene,[1,45,144,145] (2) hexatriene,[1,45,122,146] (3) octatetraene,[1,45,119,140] (4) decapentaene,[1,41,148] (5) retinol,[12] (6–8) retinal in various solvents,[12] (9) diphenyloctatetraene,[125,149] (10) dimethyltridecahexaene,[42] (11) homologue of β-carotene ($C_{30}H_{44}$),[12] (12) amphothericin B,[12,147] (13) homologue of β-carotene ($C_{35}H_{50}$),[12] (14) crocetin,[12] (15) β-carotene,[12] (16) lycopene,[12] (17) bixin,[12] (18) capsanthin,[12] (19) homologue of β-carotene ($C_{50}H_{68}$),[12] (20) homologue of β-carotene ($C_{60}H_{80}$),[12] (21) *N*-dodecapentaenylidinebutylamine,[47,134] (22) dodecapentaenal.[126] The solid and dashed curves are obtained from eq 5 for constant V and Δ. Solid line: $V = 1840$ cm^{-1}, $\Delta = 4000$ cm^{-1}. Dashed line: $V = 2015$ cm^{-1}, $\Delta = 0$ cm^{-1}.

calculated excitation energy goes down from 4.53 eV (for C_6) to 2.68 eV (for C_{36}). Vibronic coupling calculations indicate that a C=C stretch mode of a_g symmetry strongly couples the $1A_g$ and $2A_g$ states. This offers a straightforward and simple explanation of the observed correlation.[86]

Vibronic coupling of the ground state with the first excited state, $2A_g$, depresses the adiabatic frequency of the active mode. This effect can be expressed by eq 5 specialized to the $1A_g$–$2A_g$ coupling. It is known that the gap between the $2A_g$ and $1B_u$ states varies only slightly (by 2000–3000 cm^{-1}) for a wide range of polyene chain lengths.[1] Neglecting this variation, we replace E_{2A_g} in eq 5 by $E_{1B_u} - \Delta$, where Δ is the average gap between the $2A_g$ and $1B_u$ states. Keeping V constant for all polyenes we get a simple dependence between ω and E_{1B_u}. Comparison of this dependence with experimental data for a large group of molecules containing polyene chains of various lengths.[1,12,41,42,47,119,122,125,126,144-149] leads to the result depicted in Figure 1 adopted from ref 86.

The values of the diabatic frequency (Ω), the vibronic coupling parameter (V), and the energy gap (Δ), used in Figure 1 are in the range of the values obtained from quantum chemical calculations.[36,37,137,140] Allowance for a modest linear variation of Δ and/or V with the excitation energy of the $1B_u$ state improves, to some extent, the correlation between the experimental data and the curve resulting from eq 5.[86] The scatter of the experimental points in the graph indicates modest variations of the energy gap and the vibronic coupling strength in individual molecules. It is found that one ground state diabatic frequency ($\Omega = 1730$ cm^{-1}), one vibronic coupling parameter ($V = 1840$ cm^{-1}), and one energy gap ($\Delta = 4000$ cm^{-1}) between the S_1 and S_2 states for any polyenic compound suffice to reproduce all the frequency changes in the C=C stretch Franck–Condon-active mode in more than 20 polyenes. The one

TABLE 13. Diabatic, Adiabatic and Experimental Frequencies (cm^{-1}) of a_g Modes of *all-trans*-Octatetraene in the $1A_g$ and $2A_g$ States (CH Stretches are Omitted)

$1A_g$			$2A_g$		
diab	adiab[a]	exptl[b]	diab	adiab[a]	exptl[c]
1714	1601[d]	1613[d]	1676	1711[d]	1754[d]
1625	1574	1608	1577	1487	
1448	1438	1423	1471	1464	
1361	1357	1299	1352	1350	
1326	1323	1291	1327	1323	
1297	1295	1281	1277	1267	1271
1223	1178[d]	1179[d]	1242	1220[d]	1219[d]
1202	1154	1136	1220	1137	
959	952	956	960	958	
595	595	538	605	604	529
338	335	343	336	334	340
264	264	242	259	259	219

[a] Reference 87. [b] Reference 118. [c] Reference 40. [d] Strongly Franck–Condon active.

TABLE 14. Diabatic, Adiabatic, and Experimental Frequencies (cm^{-1}) of a_g Modes of *all-trans*-Decapentaene in the $1A_g$ and $2A_g$ States (CH Stretches Are Omitted)

$1A_g$				$2A_g$			
diab	adiab[a]	γ^b	exptl[c]	diab	adiab[a]	γ^b	exptl[c]
1718	1575[d]	1.2	1598[d]	1689	1710[d]	1.9	1737[d]
1658	1608	0.3	–	1638	1511	0.1	1528
1556	1541	0.1	–	1494	1475		–
1431	1425		–	1403	1379		–
1365	1359		–	1360	1354		1357
1341	1338		–	1323	1319		–
1309	1305		–	1286	1163	0.1	–
1283	1278		1288	1264	1254	0.2	1282
1221	1175[d]	0.9	1181[d]	1228	1202[d]	0.5	1240[d]
1192	1152	0.3	1147	1216	1212	0.2	1256
945	936		–	950	948		–
648	646		–	643	642		–
476	476		436	465	467		–
273	270	0.1	256	272	271	0.1	–
181	180		–	180	180		–

[a] Reference 88. [b] $\gamma = B^2/2$, where B is the dimensionless displacement parameter of the mode for the $2A_g \rightarrow 1A_g$ (third column) and $1A_g \rightarrow 2A_g$ (seventh column) transitions, respectively; only $\gamma \geq 0.1$ are reported. [c] Reference 41. [d] Strongly Franck–Condon active.

case (nystatin molecule; vide infra) that does not fit is explained in terms of interaction between two polyenic chains;[150] once the effect of the interaction is removed, its two Franck–Condon-active C=C stretch frequencies fit into the same pattern.

6. Quantum Chemical Calculations of S_0 and S_1 Diabatic and Adiabatic Frequencies

Because of their simplicity, semiempirical quantum chemical methods are suited to introduce and develop new procedures. The QCFF/PI[16,17] model was selected to calculate all the quantities used as input for the diabatic model for polyenes. This method includes an empirical force field for σ-electrons and parametrizes the π-electrons quantum chemically. In its original formulation, this program was devised to yield ground- and excited-state geometries of conjugated systems. A special effort was made to devise an efficient and approximate algorithm to obtain reliable data on the electronic ground-state normal modes and frequencies. This algorithm was based on the neglect of electron density derivatives with respect to the nuclear displacements and on a perturbation correction in terms

TABLE 15. Diabatic, Adiabatic, and Experimental Frequencies (cm^{-1}) of a_g Modes of *all-trans*-Dodecahexaene in the $1A_g$ and $2A_g$ States (CH Stretches Are Omitted)

$1A_g$				$2A_g$			
diab	adiab[a]	γ^b	exptl[c]	diab	adiab[a]	γ^b	exptl[c]
1724	1565[d]	1.0	1576[d]	1698	1722[d]	1.8	1779[d]
1684	1613	0.2	–	1661	1523	0.1	1616
1599	1565	0.2	–	1566	1499	0.1	–
1445	1434		–	1465	1450		–
1371	1365		–	1368	1365		–
1363	1361		–	1363	1357		–
1338	1333		–	1322	1316		–
1306	1302		–	1301	1291		–
1271	1264		–	1290	1253		–
1229	1170	0.1	1180	1253	1234[d]	0.5	1277[d]
1222	1158[d]	0.8	1152[d]	1228	1162	0.2	–
1202	1179	0.2	1180	1215	1202	0.2	1252
949	942		–	952	949		–
626	623		–	627	623		–
565	564		–	572	568		–
364	363		–	361	361		–
229	228		–	229	228		–
130	130		–	130	130		–

[a] Reference 88. [b] $\gamma = B^2/2$, where B is the dimensionless displacement parameter of the mode for the $2A_g \rightarrow 1A_g$ (third column) and $1A_g \rightarrow 2A_g$ (seventh column) transitions, respectively; only $\gamma \geq 0.1$ are reported. [c] Reference 42. [d] Strongly Franck–Condon active.

TABLE 16. Diabatic, Adiabatic, and Experimental Frequencies (cm^{-1}) of a_g Modes of *all-trans*-Tetradecaheptaene in the $1A_g$ and $2A_g$ States (CH Stretches Are Omitted)

$1A_g$				$2A_g$			
diab	adiab[a]	γ^b	exptl[c]	diab	adiab[a]	γ^b	exptl[c]
1727	1552[d]	1.0	1555[d]	1702	1716[d]	1.5	1782[d]
1698	1610		1637	1677	1555		1583
1631	1575	0.1	1596	1616	1519	0.1	1543
1547	1528		–	1489	1457		1504
1437	1430		–	1420	1396		1445
1374	1367		–	1371	1366		–
1355	1354		–	1353	1351		–
1342	1339		1336	1323	1315		1304
1319	1314		–	1303	1280		–
1301	1298		1288	1286	1265		–
1262	1253		1251	1258	1189		–
1222	1151[d]	0.9	1148[d]	1238	1233[d]	0.5	1250[d]
1212	1151	0.1	1215	1230	1207		–
1208	1159		1169	1217	1173	0.2	1177
951	944		–	953	950		–
661	660		–	658	658		–
552	548		–	547	545		–
494	493		–	488	489		–
284	283		269	284	282		–
198	197		193	198	197		–
98	98		–	98	98		–

[a] Reference 88. [b] $\gamma = B^2/2$, where B is the dimensionless displacement parameter of the mode for the $2A_g \rightarrow 1A_g$ (third column) and $1A_g \rightarrow 2A_g$ (seventh column) transitions, respectively; only $\gamma \geq 0.1$ are reported. [c] Reference 43. [d] Strongly Franck–Condon active.

of polarizability. This made the QCFF/PI Hamiltonian an excellent tool to study resonance Raman spectra, if both the Dushinsky effect and the Herzberg–Teller effect were absent. Later, Karplus and co-workers[7] included doubly excited configurations with the purpose of handling $2A_g$ states of polyenes. However, the approximation to the calculation of the force field was retained for the excited states, although its validity is not proved in this case. In fact, the A_g C=C stretch frequency inversion upon the $S_0 \rightarrow S_1$ excitation was not reproduced.[7] In our upgrading of this Hamiltonian,

TABLE 17. Diabatic, Adiabatic, and Experimental Frequencies (cm^{-1}) of a_g Modes of *all-trans*-Hecadecaoctaene in the $1A_g$ and $2A_g$ States (CH Stretches Are Omitted)

$1A_g$				$2A_g$			
diab	adiab[a]	Y[b]	exptl[c]	diab	adiab[a]	γ[b]	exptl[c]
1729	1550[d]	1.5	1555[d]	1708	1708[d]	2.5	1779[d]
1707	1579	0.2	1576	1689	1515	0.2	1511
1656	1611		1628	1639	1573		1552
1582	1554		-	1553	1488		-
1444	1433		-	1458	1449		-
1377	1373		-	1383	1378		-
1376	1369		-	1375	1370		-
1357	1354		-	1354	1350		-
1341	1337		-	1326	1315		-
1311	1307		-	1305	1302		-
1292	1287		1264	1305	1291		-
1257	1249		-	1274	1248		1292
1244	1191		1218	1250	1191		-
1222	1149[d]	1.5	1135[d]	1233	1226[d]	0.6	1246[d]
1216	1183	0.1	1164	1226	1214	0.2	1233
1199	1158		1149	1212	1155	0.2	1171
951	943		-	952	947		-
671	670		-	669	667		-
580	579		-	589	585		-
489	485		-	489	485		-
412	412		-	411	410		-
226	226		-	226	224		-
174	173		145	174	174		163
76	76		76	76	75		67

[a] Reference 88. [b] $\gamma = B^2/2$, where B is the dimensionless displacement parameter of the mode for the $2A_g \rightarrow 1A_g$ (third column) and $1A_g \rightarrow 2A_g$ (seventh column) transitions, respectively; only $\gamma \geq 0.1$ are reported. [c] Reference 44. [d] Strongly Franck–Condon active.

we corrected the approximations and devised a simple method that could handle any kind of excitation and multiplicity (see Appendix C). It was then possible to calculate both diabatic and adiabatic frequencies: the latter calculation was performed through numerical differentiation of the energy, or, introducing another approximation, by numerical differentiation of diabatic gradients (a discussion of this approximation is presented in ref 87).

In Tables 13–17, we show the adiabatic and diabatic frequencies of S_0 and S_1 for a number of polyenes,[87,88] together with their γ-parameter, which determines the Franck–Condon activity of each mode in the spectrum (see Appendix D). The difference between the diabatic and adiabatic frequency is a measure of the strength of the vibronic coupling induced by the corresponding mode. The adiabatic frequencies account very well for the observed frequencies both in the S_0 and S_1 states. These appear to be the first quantum chemical calculations that reproduce quantitatively the frequency increase of the C=C stretch mode upon excitation to the $2A_g$ state in polyenes. Recently, this anomalous frequency increase was reproduced also by ab initio calculations at the MCSCF level in butadiene, hexatriene, and octatetraene.[39] Notice that only two modes are strongly active in the absorption and emission spectra of polyenes (see Tables 13–17). The different γ, predicted for the C—C and C=C stretch modes in absorption and emission, imply a substantial amount of Dushinsky effect, which increases with the chain length and should be observable in resonance Raman spectra.

A different insight into the effect of electronic excitation and vibronic coupling can be obtained through the examination of force fields expressed in internal coordinates. Since quantum chemical methods are usually formulated in terms of Cartesian coordinates, this requires rotation of the Hessian matrix (see Appendix E). In Table 18, we show the adiabatic and diabatic CC stretch force constants for the model compound *s-trans*-decapentaene. It is apparent that the electronic excitation affects only the diagonal CC force constants and in the most predictable way, namely it increases the C—C and decreases the C=C force constants. The introduction of vibronic coupling affects also off-diagonal elements of the C_nC_{n+1} type. In addition it emerges that the electronic excitation is localized at the center of the molecule. This result is confirmed by the comparison of the S_0 and S_1 equilibrium geometries. The S_0 and S_1 equilibrium CC bond lengths of a number of polyenes, from octatetraene to hexadecaoctaene, are listed in Table 19. As can be seen, CC bond length changes upon excitation amount to an inversion of the bond length alternation with respect to S_0. While in the shorter polyenes these changes extend over the entire molecule, in the longer polyenes they are limited to the central section of the carbon chain, resulting in two regions where inversion of bond alternation occurs. These regions are both characterized by at least two adjacent CC single bonds

TABLE 18. Adiabatic (Diabatic) CC Stretch Force Constants (mdyn/Å) of *all-trans*-Decapentaene (from ref 88)

	C_1C_2	C_2C_3	C_3C_4	C_4C_5	C_5C_6
			S_0		
C_1C_2	8.420 (8.659)				
C_2C_3	0.718 (0.407)	5.210 (5.944)			
C_3C_4	-0.099 (0.005)	0.684 (0.408)	7.897 (8.258)		
C_4C_5	0.044 (-0.001)	-0.065 (0.002)	0.741 (0.408)	5.248 (6.044)	
C_5C_6	-0.016 (-)	0.041 (-0.001)	-0.122 (0.004)	0.737 (0.408)	7.821 (8.212)
C_6C_7	0.008 (-)	-0.012 (-)	0.050 (-0.001)	-0.079 (0.002)	0.737 (0.408)
C_7C_8	0.001 (-)	0.007 (-)	-0.019 (-)	0.050 (-0.001)	-0.122 (0.004)
C_8C_9	0.002 (-)	-0.002 (-)	0.007 (-)	-0.012 (-)	0.041 (-0.001)
C_9C_{10}	0.003 (-)	0.002 (-)	0.001 (-)	0.008 (-)	-0.161 (-)
			S_1		
C_1C_2	6.435 (7.803)				
C_2C_3	1.308 (0.404)	6.072 (7.030)			
C_3C_4	0.212 (0.004)	0.512 (0.404)	5.670 (6.448)		
C_4C_5	-0.126 (-0.001)	0.121 (0.003)	0.343 (0.404)	7.151 (7.437)	
C_5C_6	0.131 (-)	-0.153 (-0.001)	0.337 (0.002)	0.367 (0.406)	6.183 (6.685)
C_6C_7	0.097 (-)	-0.044 (-)	-0.025 (-0.001)	0.219 (0.003)	0.367 (0.406)
C_7C_8	0.220 (-)	-0.111 (-)	-0.097 (-)	-0.025 (-0.001)	0.337 (0.002)
C_8C_9	-0.231 (-)	0.132 (-)	-0.111 (-)	-0.044 (-)	-0.153 (-0.001)
C_9C_{10}	0.365 (-)	-0.231 (-)	0.220 (-)	0.097 (-)	0.131 (-)

TABLE 19. Equilibrium CC Bond Lengths (in Å) of *all-trans*-Hexatriene (C_6), Octatetraene (C_8), Decapentaene (C_{10}), Dodecahexaene (C_{12}), Tetradecaheptaene (C_{14}), and Hexadecaoctaene (C_{16}) in the S_0 ($1A_g$) and S_1 ($2A_g$) States[a]

	bond	S_0	S_1		bond	S_0	S_1
C_6	C_1C_2	1.347	1.444	C_{14}	C_1C_2	1.348	1.361
	C_2C_3	1.464	1.390		C_2C_3	1.458	1.427
	C_3C_4	1.360	1.450		C_3C_4	1.364	1.421
C_8	C_1C_2	1.347	1.409		C_4C_5	1.453	1.386
	C_2C_3	1.463	1.389		C_5C_6	1.367	1.439
	C_3C_4	1.361	1.450		C_6C_7	1.451	1.390
	C_4C_5	1.459	1.395		C_7C_8	1.368	1.430
C_{10}	C_1C_2	1.347	1.386	C_{16}	C_1C_2	1.347	1.356
	C_2C_3	1.464	1.400		C_2C_3	1.458	1.436
	C_3C_4	1.361	1.447		C_3C_4	1.364	1.408
	C_4C_5	1.459	1.388		C_4C_5	1.452	1.394
	C_5C_6	1.363	1.436		C_5C_6	1.367	1.436
C_{12}	C_1C_2	1.347	1.371		C_6C_7	1.451	1.385
	C_2C_3	1.461	1.414		C_7C_8	1.368	1.429
	C_3C_4	1.363	1.436		C_8C_9	1.450	1.390
	C_4C_5	1.455	1.383				
	C_5C_6	1.365	1.438				
	C_6C_7	1.454	1.391				

[a] From refs 87, 88.

TABLE 20. Computed a_g Vibrational Frequencies (cm^{-1}) of *trans*-Hexatriene and of TMB in the T_1 State (CH Stretches Are Omitted)

hexatriene[a]		TMB[b]	
ω	description	ω	description
1554[c]	C—C, C=C	1572[c]	C—C, C=C
1483	CH_2 sciss	1464	CH_3 def
1369	CH rock (C=C)	1459	CH_3 def
1321	CH rock (C–C)	1441	CH_3 def
1193	C=C (C—C)	1436	CH_3 def
1154[c]	C=C	1353[c]	CH rock, C–C, C–CH_3
939	CH_2 rock	1311[c]	C=C, C—C
448	CCC bend	1186	C–CH_3, C–C
385	CCC bend	1015	CH_3 rock
		967	CH_3 rock
		835	C–CH_3
		534	CCC bend
		360[c]	CCC bend
		291	CCC bend

[a] Reference 89. [b] Reference 90. [c] Modes with strong Franck–Condon activity.

and can be associated to a nonbonding electron. Therefore equilibrium geometries suggest that the S_1 state in long polyenes corresponds to two neutral solitons[151] located in the regions of the inversion of bond alternation.

7. Triplet-State Vibrations and Conformations

In this section we review the time-resolved resonant Raman spectra of short polyenes obtained recently and the information derived from their interpretation about the potential energy surface and the properties of different configurational and conformational isomers in the T_1 state.

In polyenes, the lowest triplet state T_1 is described by the HOMO → LUMO configuration. In C_{2h} symmetry, its wave function is classified as 1^3B_u. As shown by Woodward–Hoffmann type diagrams, this state has a flat potential energy surface along the C=C torsion, in sharp contrast with the S_0 state energy surface which has a barrier of roughly 50 kcal/mol at the twisted geometry. The flat potential energy surface of the T_1 state opens an efficient decay channel in polyenes via cis–trans isomerization. This new channel operates side

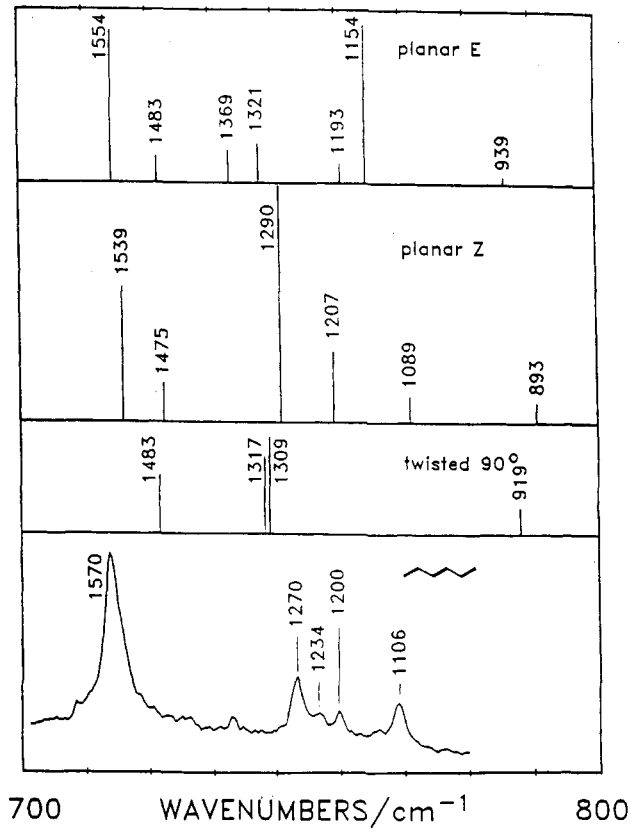

Figure 2. Calculated T_1 state frequencies and resonance Raman intensities of the totally symmetric modes of trans (*E*), cis (*Z*), and twisted forms of hexatriene together with its observed T_1 resonance Raman spectrum.[89] The intensities are taken proportional to the γ-values of the $T_1 \rightarrow T_n$ transition (n = 5 and 6 for planar and twisted forms, respectively).

by side with the normal $T_1 \rightarrow S_0$ intersystem crossing (isc) that proceeds at the trans geometry. In fact, the molecule in the T_1 state can be regarded as moving freely along the torsional coordinate, in particular it can reach easily the twisted geometry where isc to the ground state takes place with a relatively high rate. This follows from the small T_1–S_0 energy gap at this geometry according to the energy gap law[152] governing radiationless transitions. After decaying from the T_1 state to the top of the S_0 state barrier, the molecule relaxes toward either the cis or the trans conformation, thus undergoing eventually isomerization. The overall photoisomerization mechanism closely resembles that of stilbene.[153] A strong experimental support for this picture and of almost free C=C torsion in T_1 is given by the lifetimes of the first triplet state of butadienic and hexatrienic derivatives which are shorter than 100 ns.[154-159] This is at odds with lifetimes of planar hydrocarbons, which are in the 10–100 ms range,[160] and is again very similar to the T_1 lifetime of stilbene.[161]

In principle, high level ab initio calculations could yield information on the finer details of the T_1 potential energy surface (PES); however, to the best of our knowledge, no calculation that explores the effect of both the size of the atomic basis set and of electron correlation on the T_1 PES is available to date. Some consensus seems to have been reached about butadiene having besides the trans minimum, a second, more stable minimum, at a structure with one of the C=C bonds rotated by 90°.[64,55,162-165] The energy difference between these two conformations is calculated to be in the 2.8 and 11.2 kcal/mol range, with the highest level

calculation yielding the smallest energy gap. Similar results have been obtained for hexatriene.[162-164,166] In this case, it is the central double bond that is twisted, and the energy gap between the 90° twisted molecule and the trans conformation is calculated to be between 1.9[164] and 6.0[163] kcal/mol. Also notice that a very recent calculation,[166] with full geometry optimization, leads to the twisted form being higher in energy by 3.8 kcal/mol.

Given the present uncertainties in the determination of barriers and minima for these molecules, it seemed best to combine spectroscopic and theoretical information in the form of observed and quantum chemically calculated resonance Raman spectra of different isomers. Time-resolved resonance Raman (RR) spectra of T_1 have been recorded for 2,5-dimethyl-2,4-hexadiene (or tetramethylbutadiene, TMB) and for hexatriene and several of its methylated and deuterated derivatives by Wilbrandt and co-workers.[158,159,167-169] These spectra have been subsequently analyzed with the help of theoretical RR spectra computed for the trans, cis and twisted isomers.[89,90,170,171] The adopted procedure was to assign as the dominant conformer the one whose calculated spectrum most closely corresponds to that observed. In this way, the PES at the more stable conformation was characterized both in terms of structural parameters and normal mode frequencies. It was possible to show that the planar conformer dominates the spectrum and the twisted conformer cannot be more stable than the trans conformer by more than 3.0 kcal/mol (vide infra). To construct the theoretical T_1 RR spectra, QCFF/PI and CNDO/S calculations were performed to identify the nature of the intense $T_1 \rightarrow T_n$ transition that gives the dominant contribution to the resonance Raman scattering. The RR activity of each totally symmetric mode, for the trans, twisted and cis conformations, was assessed through the QCFF/PI calculation of T_1 and T_n equilibrium structures and normal mode frequencies.

7.1. Hexatriene

The computed T_1 vibrational frequencies of the a_g modes are reported in Table 20.[89] They are quite different from those in the S_0 state; in particular, the a_g CC stretch mode of highest frequency has a lower frequency in the T_1 than in the S_0 state, in sharp contrast with its behavior in the S_1 and S_2 states. Only one intense $T_1 \rightarrow T_n$ transition has been predicted at any geometry along the torsional coordinate. It was found at 4.32 and 5.49 eV[89,170] for the trans and twisted molecule, respectively, while the corresponding transient absorption spectrum was observed at 315 nm (3.94 eV).[155,158] This transition is the main source of the intensity of the T_1 RR spectra of hexatriene. The observed and calculated T_1 RR spectra are shown in Figure 2.[89,159,170] It was found that the RR spectra of *cis*- and *trans*-hexatriene coincide. This was assumed to mean either that a common minimum is reached on the T_1 PES by the two isomers or that equilibrium population of different minima is reached within the pump-probe delay of the experiment (60 ns). Under the assumption that the photoisomerization is adiabatic, i.e., that no surface crossing occurs, the upper limit to the barrier height along the isomerization path in T_1 was found to be less than 7.6 kcal/mol.[89] A comparison of the spectra showed that the planar conformers are

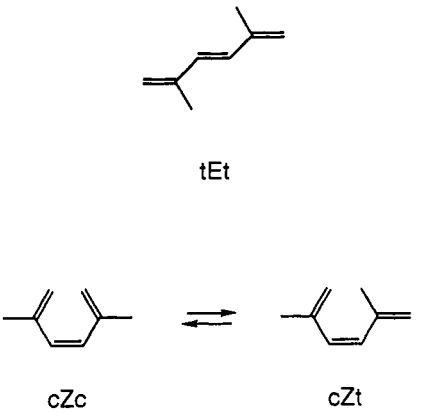

Figure 3. Structure of the dominating conformers of the trans (*E*) and cis (*Z*) forms of 2,5-dimethylhexatriene.

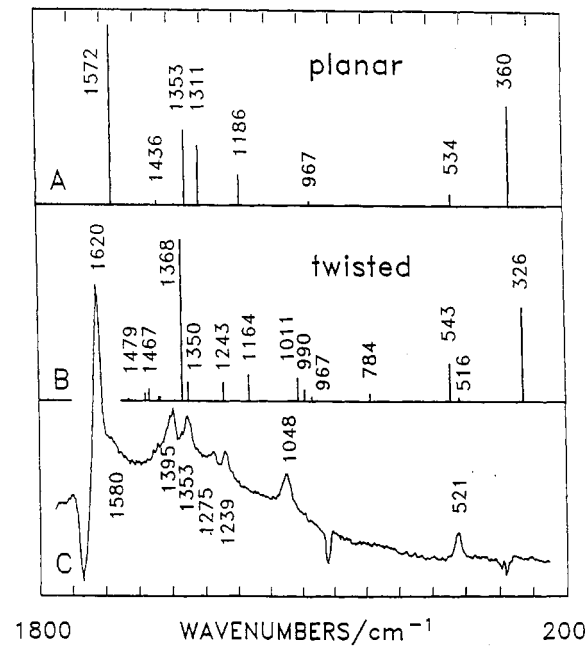

Figure 4. Calculated T_1 state frequencies and resonance Raman intensities of the totally symmetric modes of planar and twisted forms of TMB together with its observed T_1 resonance Raman spectrum.[90] The intensities are taken proportional to the γ-values of the $T_1 \rightarrow T_n$ transition (n = 4 and 5 for planar and twisted forms, respectively).

the dominant contributors to the RR spectrum. Notice that the twisted species will be in preresonance while the planar isomers will be in resonance. It was estimated that the efficiency of the resonance scattering is about 2000 times that of the preresonance scattering for the twisted form. This together with the observed spectrum indicated an upper limit of 2.7 kcal/mol[89] for the energy difference between the trans and twisted conformers on the T_1 potential energy surface. This conclusion was supported by an analysis of transient RR spectra of a number of methylated and deuterated derivatives of hexatriene.[170,171]

A study of 2,5-dimethylhexatriene yielded information on the torsion about CC single bonds in the T_1 state. Both *E* and *Z* isomers were considered.[169,170] While in the *E* isomer the tt conformer dominates, the *Z* isomer in the S_0 state reaches thermal equilibrium between the tc and the cc conformers (see Figure 3). Since the T_1 RR spectra of the two isomers are different,[169] it was concluded that the conformers do not

equilibrate in the T_1 state, but retain their ground-state distribution. Thus the principle of nonequilibration of excited rotamers (NEER), originally formulated for singlet excited states,[172,173] is found to apply also to the T_1 state of hexatriene. This implies that the barrier to single bond rotation in the T_1 state is larger than 7.6 kcal/mol.[89,170]

7.2. Tetramethylbutadiene

Computed vibrational frequencies of the a_g modes of *trans*-TMB in the T_1 state are reported in Table 20.[90] A comparison of calculated and observed[167] T_1 RR spectra is shown in Figure 4. It appears that the trans isomer dominates this spectrum since the strong 1620 cm^{-1} band apparently corresponds to the normal mode of 1562 cm^{-1} frequency calculated for the trans isomer. Notice that no bands are predicted in this region for the twisted form of either butadiene or TMB. In the entire spectrum, only the 1275 cm^{-1} band cannot be assigned to a Franck–Condon-active mode of the trans conformer. If it belongs to the twisted form, the relative population of the two forms can be estimated. Once the corrections for the preresonance condition of the nonplanar form and the different Franck–Condon activity of the modes are considered, the population of the twisted form turns out to be at most 30 times larger than that of the trans conformer, implying an energy gap between the two molecules smaller than 2 kcal/mol. This estimate is close to that obtained for hexatriene and suggests that for short polyenes the trans and twisted forms are energetically close.

Other polyenic systems in their T_1 state have been studied by transient RR spectroscopy, including several isomers of β-carotene,[168] β-apo-8′-carotenal,[175] and isomeric retinal and its homologues.[176,177] Theoretical analysis of the T_1 RR spectra of these compounds along the lines followed for TMB and hexatriene will be necessary to extract unambiguous information from the spectra.

8. Spectroscopy of Ethylene

The ethylene molecule is the basic building stone of all polyenes. Despite its simplicity, its spectroscopy is complicated by the strong coupling of the π-electrons to the σ-electron core upon electronic excitation. Theoretical and spectroscopic evidence indicate that ethylene twists by 90° about the C=C bond upon $\pi\pi \rightarrow \pi\pi^*$ excitation (see ref 178). Thus, whereas the ground state, N, belongs to the D_{2h} point group symmetry, the lowest excited singlet state, V, and triplet state, T, have equilibrium configurations of the D_{2d} symmetry. The twisting of the molecule arises because the $\pi \rightarrow \pi^*$ excitation turns the interaction between the two atomic p orbitals from bonding to antibonding, resulting in a molecule that relaxes to a staggered equilibrium configuration in which the p orbitals become orthogonal. The twisting around the C=C bond leads to a decrease in the bond order and to a larger CC bond length in the excited states. As a result one expects that the vibronic structure of the N → V and N → T transitions should be dominated by the torsional (ν_4) and CC stretching (ν_2) modes.

The N → V transition has been investigated experimentally by a number of authors.[179-182] It shows a long and somewhat irregular progression of bands of ever increasing intensity on a low-energy side of an intense transition to the first Rydberg state, R.[183] The origin of the N → R transition appears at 174.4 nm[179,180,183] and the observed part of the N → V transition extends down to more than 9000 cm^{-1} below this origin. The diffuse bands have a mean spacing of ca. 800 cm^{-1} in normal ethylene. In fully deuterated ethylene, the line width is much smaller and these bands split into multiplets of narrow peaks separated by ca. 170 cm^{-1}.

The spin-forbidden N → T transition was recorded with reasonable resolution by means of the energy-loss spectrum of scattered electrons.[184] This spectrum should have the same vibrational structure as the corresponding optical absorption spectrum which is too weak to be resolved meaningfully.[185,186] Note that the N → T absorption spectrum may differ from the energy-loss one because of the presence of spin–orbit induced components coming from a singlet state with a very different equilibrium geometry than the lowest triplet of ethylene.[187] The N → T vibrational structure consists of a long, Poisson-like progression of peaks separated by ca. 1000 cm^{-1}. Each peak possesses a secondary fine structure with an intensity pattern that varies systematically along the progression.

Ab initio calculations of the ethylene geometries and force fields in the N, V, and T states have been used to clarify the structure of the transitions.[188-193] The calculations of the force fields of the ground and triplet states were performed[191] with the GAMESS program[194] at the RHF level for the N state and at the UHF level for the T state with the 6-31++G** basis set.[195,196] The HONDO program[197] at the ROH/6-31+G* level[195,196] was used[193] to evaluate the geometry and force field of the V state. A summary of these calculations is presented in Table 21.

Three things emerge clearly from Table 21. First, the energy barriers for torsion are very different in the V and T states. Second, the ν_3 totally symmetric mode that corresponds to the scissoring motion of the CH_2 group should become Franck–Condon active in the spectra due to mixing with the ν_2 C=C stretch mode upon excitation. Third, the displacement parameters of these two totally symmetric modes are very different in the two transitions. Thus the ab initio calculations

TABLE 21. Calculated Vibrational Frequencies, Displacement Parameters, and Energy Barriers for Torsion in the N, V, and T States of Ethylene

	state		
parameter	N	V	T
E_b^a	20900[b]	12600 (15250)[c]	5025
ω_2^d	1647[e] (1630)[f]	1520[e,g] (1373)[e,h]	1440[e,g] (1432)[e,h]
B_2^i		1.21[g] (0.49)[h]	0.68[g] (0.43)[h]
ω_3^j	1332[e] (1344)[f]	972[e,g] (939)[e,h]	1002[e,g] (1050)[e,h]
B_3^i		0.91[g] (1.18)[h]	3.07[g] (2.25)[h]
ω_4^k	1022[e] (1027)[f]	573i[e,g,l] (607)[e,h]	552i[e,g,l] (574)[e,h]

[a] Energy barrier for 90° rotation (cm^{-1}). [b] Value obtained from fitting torsional levels obtained in resonance Raman scattering—refs 197, 198. [c] Value obtained from fitting the fine structure of the N → V transition in fully deuterated ethylene—ref 192. [d] Frequency of the C=C stretching mode cm^{-1}. [e] Ab initio value scaled down by a factor of 0.9. [f] Experimental value—ref 199. [g] D_{2h} conformation. [h] D_{2d} conformation. [i] Displacement parameter for the transition from the ground state (dimensionless). [j] Frequency of the CH_2 scissors cm^{-1}. [k] Frequency of the torsional mode cm^{-1}. [l] Imaginary frequency indicates unstable configuration.

indicate that the vibrational structure of the two transitions may be quite different. Modeling of this structure based on parameters obtained from ab initio methods supports these conclusions.[192,193]

The displacement parameters of ν_2 and ν_3 modes in the N → V transitions are small, so that their Franck–Condon progressions are short and the origin band is the strongest member. On the other hand, the torsional mode (ν_4) forms a long progression of the 4_n^{n+2k} transitions due to the rotated geometry of the excited state. The intensity of these transitions peaks for the final levels located near the top of the torsional barrier of the excited state, i.e., for levels whose wave functions are localized near the planar geometry of the ground electronic state. Since the observed spectrum corresponds to levels located well below the top of the barrier of the V state, the recorded torsional progression has an intensity distribution such that the intensity increases rapidly with k. Therefore, the structure resulting from ν_2 and ν_3 modes is hidden in the room temperature spectra under much stronger torsional transitions which occur in the same energy region. Thus the totally symmetric modes play no role in the visible structure of this transition. On the other hand, the hot bands starting from excited levels of the torsional mode contribute significantly to this structure. This arises because the 4_1^{2n+1} transition, which occurs at roughly the same energy as 4_0^{2n} (the mean separation between them is ca. 170 cm^{-1} in fully deuterated ethylene), has so much larger intensity, that even after correction for the Boltzmann factor it contributes to the same extent to the absorption spectrum. The well-resolved spectrum of fully deuterated ethylene clearly shows the presence of hot bands. The other interesting feature of its vibrational structure is the cold-band progression separated from the 4_0^{2n} progression by ca. 150 cm^{-1}.[180,181] It has been assigned as the induced progression resulting from vibronic coupling between the V state and the first Rydberg state R by the ν_8 mode of b_{2g} symmetry.[193] This assignment is supported by the observation of the resonance Raman fundamental located at 924 cm^{-1} in the spectrum obtained with 184-nm excitation[199] (the experimental frequency of the ν_8 mode listed in ref 200 is 940 cm^{-1}).

The N → T transition, on the other hand, is dominated by the totally symmetric modes while the torsional mode is responsible for the poorly resolved fine structure of the main bands.[192] The backbone of the vibrational structure is formed by the ν_3 mode, which possesses a very large displacement parameter for this transition (see Table 21). The ν_2 and ν_3 modes mix heavily upon excitation to the T state. This is evidenced by very different displacement parameters of these modes for the N → T and T → N transitions.[192] The displacement parameter of the ν_3 mode depends on the torsional angle—it decreases by ca. 30% upon going from the D_{2h} to the D_{2d} configuration. This indicates coupling between the ν_3 and ν_4 modes in the T state. It was shown that this coupling is responsible for a systematic change in the intensity distribution of the fine structure of the spectrum along the progression associated with the ν_3 mode.[192]

The structure of the N → R transition shows activity of the ν_2 and ν_4 modes. The torsional transitions consist of the 4_i^j bands where i = 0, 1 and j = 1, 2.[179,180] Their appearance results from a slight twist of the R state torsional potential.[183,201] The potential minimum occurs at the torsional angle, Θ, of ca. 23°, where Θ = 0° corresponds to the planar configuration. The barrier height at this configuration is less than 280 cm^{-1}, so that only the zero-point level of (normal) ethylene lies below the top of the barrier. The 4_0^0 and 4_0^2 bands form a doublet whose separation decreases and the intensity shifts more and more into the latter band with the increasing level of deuteration.[180,183] These changes can be entirely accounted for by systematic variation of the moment of inertia for the torsional motion among the isotopomers of ethylene.[201] The observed energy separations between the 4_0^0 and 4_0^2 transitions in higher Rydberg states (ns, 3p, ndσ, and ndδ)[202] indicate that the torsional potential is essentially the same in these states. Although only one a_g mode, ν_2, seems to be active in the intense N → R transition, resonance Raman spectra taken in that region[199,203] indicate activity of two totally symmetric modes, namely, ν_2 and ν_3. It has been shown that the resonance Raman activity of the ν_3 mode results from a strong mode mixing (Dushinsky effect) between the C=C stretch and the CH_2 scissors upon electronic excitation.[201]

Resonance Raman spectra taken in the region of the V and R states[199,203] show a progression that can be clearly identified with the fundamental and with odd quantum overtones of the torsional mode. This is surprising at first sight since in the planar geometry torsion is of *ungerade* character and therefore these bands should be strictly forbidden. However, ethylene is a flexible molecule whose excited-state geometry is different than that of the ground state. In such a situation, the dynamic double group $G_{16}^{(2)}$ should be used to describe the symmetry of excited states.[204] In this case, the optical selection rules are identical with those of the D_2 point group, allowing formally for the appearance of the fundamental and odd overtones of the torsional mode in the spectra. The source of the intensity for this progression remains to be established.

9. Spectroscopy of Polyenes

Absorption spectra of polyenes are dominated by a very intense transition with a rich vibrational structure. This transition is recognized as $1A_g \rightarrow 1B_u$ (see ref 1 and those cited therein). The center of gravity of the absorption spectrum belonging to this transition shifts monotonically toward lower energy as the polyene length increases. Thus it shifts from 5.91 eV in butadiene[144,205] to 3.65 eV in dodecahexaene.[148] This energy is sensitive to interactions with solvents; for a molecule in hexane solvent, it is 2000–3000 cm^{-1} lower than for an isolated molecule.[1] The vibrational structure of the spectrum is formed by two totally symmetric modes: a double bond stretching mode with a frequency of ca. 1600 cm^{-1} and a single bond stretching mode at ca. 1200 cm^{-1}. The activity of these modes arises due to large bond-order changes upon electronic excitation which cause a noticeable exchange of character between double and single CC bonds.[18,88,89,150] The calculations of the optimized geometries by a modified QCFF/PI method[16,17] indicate that upon excitation to the $1B_u$ state, the differences between the lengths of the double and single CC bonds are greatly reduced. Quantum chemical calculations identify the $1B_u$ state as arising from the excitation of a single electron from the highest

occupied π-orbital to the lowest unoccupied π^*-orbital, i.e., a HOMO → LUMO excitation.[206]

Fluorescence is absent from butadiene and hexatriene. It is however well-known in longer polyenes. Among unsubstituted polyenes, octatetraene has the largest fluorescence quantum yield (0.6).[1] The origin of the fluorescence spectrum is shifted by ca. 0.2–0.4 eV toward lower energies from the origin of the intense absorption spectrum described above. The solvent dependence of the origin of the emission spectra is much weaker than that of the absorption.[32,207] Also the vibrational structure of the emission is different than that of the absorption. These two facts indicate that the emitting state is not the $1B_u$ state. This is confirmed by two-photon absorption studies[40,49-52] which prove that the emitting state is of *gerade* symmetry. This state is identified with the $2A_g$ state. Again, the same two totally symmetric stretches dominate the spectrum; however, the displacement parameters of these modes for the $1A_g \rightarrow 2A_g$ transition are much larger than those for the $1A_g \rightarrow 1B_u$ transition. Calculations performed at the optimized geometries of the two states, which produce the energies of the 0–0 transitions, place the $2A_g$ state origin below that of the $1B_u$ state. Thus the potential surfaces of the two states cross along the totally symmetric coordinates (conical intersection) so that the ordering of the states depends on the geometry. The minimum of the potential surface of the $2A_g$ state lies however below the minimum of the potential surface of the $1B_u$ state. The conical intersection of the two surfaces results from the much larger displacement parameters of the totally symmetric modes, and therefore the Stokes' shift, for the $1A_g \rightarrow 2A_g$ transition than for the $1A_g \rightarrow 1B_u$ transition. Quantum chemical calculations of the optimized $2A_g$ state geometry of longer polyenes[87,88] indicate that excitation to this state effectively interchanges the CC bonds, double bonds becoming single and vice versa.

9.1. Butadiene

The electronic structure of the excited states of butadiene has been studied extensively in a number of ab initio calculations.[38,39,60,61,64-68] They indicate that the lowest excited state is of $2A_g$ symmetry. Proper geometry optimization and inclusion of at least doubly excited configurations is essential for arriving at this conclusion. Calculations performed with the ground-state geometry yield the $1B_u$ state as the lowest excited singlet. Optimization of the geometry of the $2A_g$ state under restriction to planarity leads to imaginary frequencies for some out-of-plane vibrations,[38,39] namely two a_u and two b_g modes connected with rotations around terminal C=C bonds and pyramidalization. The fully optimized geometry of this state indicates nonplanar structures of C_2 and S_2 symmetries, separated by a barrier of ca. 1600 cm^{-1}.[38] Attempts to locate experimentally the origin of the $2A_g$ state were so far unsuccessful, although the recent location of this origin for hexatriene[59] suggests that this situation will change soon.

Resonance Raman scattering below the threshold of the $1B_u$ manifold indicates resonance enhancement of the overtone of the ν_{24} mode of b_u symmetry.[58] This enhancement vanishes in the region of the $1A_g \rightarrow 1B_u$ transition. It has been interpreted as a resonance enhancement from the $2A_g$ state. The mechanism of enhancement is supposed to be vibronic coupling between the $2A_g$ and $1B_u$ states by this lowest frequency skeletal bending b_u mode.

The absorption spectra of butadiene, butadiene-d_2, butadiene-d_4, and butadiene-d_6 corresponding to the $1A_g \rightarrow 1B_u$ transition have been extensively studied both experimentally[53,107,205,207,208] and theoretically.[7,80,208,209] This absorption starts at ca. 46 200 cm^{-1}. It consists of four wide bands separated by 1430–1550 cm^{-1}, depending on the isotopomer. The width of these bands varies from 560 cm^{-1} in butadiene to 430 cm^{-1} in butadiene-d_6.[53] The high-energy tail of the absorption is contaminated by a series of Rydberg transitions ($\pi \rightarrow 3s$, $\pi \rightarrow 3p$, and so on).[207] Semiempirical calculations[7,209] based on the QCFF/PI method[16,17] indicate that the vibrational structure of the $1A_g \rightarrow 1B_u$ transition is due solely to the change of the CC bond lengths upon HOMO → LUMO excitation. The double bond stretching mode, ν_4, provides the backbone for this structure. Excitation of normal and externally deuterated butadiene mixes heavily the C–C stretch, ν_6, with the CH wag, ν_7, making the wagging mode the second strongest Franck–Condon-active mode for this transition in these isotopomers. Butadienes with inner hydrogen atoms replaced by deuterium retain the identity of their totally symmetric modes upon electronic excitation.[209] Small variations in the relative intensities of the vibrational bands (0–0, 0–1, and 0–2) between the four isotopomers observed in the spectra are well reproduced by quantum chemical calculations. The calculated displacement parameters[209] for the ν_4, ν_7, and ν_9 modes agree reasonably well with those determined from the preresonance Raman excitation profiles of the totally symmetric fundamentals (1.49 vs 1.44, 0.94 vs 0.76, and 0.44 vs 0.61, respectively).[107] Some difference in the two values of the displacement parameters of the C–C stretch (ν_6) mode (0.52 vs 0.2) may result from the neglect of ν_6–ν_7 mode mixing in the analysis of the excitation profiles. The total Stokes' shift for the $1A_g \rightarrow 1B_u$ transition is calculated to be ca. 2400 cm^{-1}, in excellent agreement with the Raman studies.

The lowest two triplet states of butadiene have been located by means of electron-impact spectroscopy.[72-74] The two singlet–triplet bands are very broad, indicating a large geometry change of the molecule upon excitation to the triplet state. The lowest triplet absorption band maximum is located at 3.22 eV. This state is identified as the 1^3B_u state. The second triplet absorption band has a maximum around 4.91 eV. It is identified as belonging to the 1^3A_g state. The vibrational structure of the singlet–triplet transitions is poorly resolved and has not been studied in any detail.

9.2. Hexatriene

Absorption spectra of *trans*- and *cis*-hexatriene corresponding to the $1A_g \rightarrow 1B_u$ and the $1A_1 \rightarrow 1B_1$ transition, respectively, have been studied in a number of experimental reports.[53,210] The spectrum of the trans isomer is much better resolved than that of the cis isomer, not only in the room temperature gas spectra but also in the spectra of jet-cooled hexatrienes. The spectrum of the trans isomer shows strong Franck–Condon activity of the two a_g modes which can be

identified as the C=C and C—C stretches with 1631 and 1224 cm^{-1} frequencies, respectively.[210] The corresponding frequencies for the cis isomer are 1618 and 1248 cm^{-1}. Also weaker Franck–Condon activity has been reported of a skeletal angle bending mode with frequencies of 313 and 389 cm^{-1} in the trans and cis isomers, respectively.

The difference in the structure of the absorption spectra of the trans and cis isomers was rationalized in terms of the Dushinsky effect.[210] It was argued that excitation to the $1B_1$ state of the cis isomer mixes the CC stretching modes with the low frequency skeletal bending mode of a_1 symmetry. Steric hindrance between two inner hydrogen atoms was presented as the reason for this mode mixing. The required mixing of the low frequency mode with the C=C stretch amounts to ca. 4.6° rotation of the normal modes.

A full theoretical analysis of the absorption spectra of the two isomers is presented in ref 85. Displacement parameters and Franck–Condon overlaps for the $1A_g \rightarrow 1B_u$ transition are calculated by using the QCFF/PI method.[16] It follows that modes ν_5 and ν_{10} of the trans isomer are the main Franck–Condon-active modes. Their calculated $1B_u$ state frequencies and displacement parameters are 1569 and 1192 cm^{-1}, and 1.42 and 0.98, respectively. The cis isomer absorption spectrum is dominated by ν_5 and ν_9 modes with calculated frequencies of 1566 and 1278 cm^{-1} and displacement parameters of 1.42 and 0.86. Secondary contributions to the vibrational structure of the absorption spectrum come from the ν_{13} mode (378 cm^{-1}, 0.42) in *trans*-hexatriene and the ν_{12} mode (417 cm^{-1}, 0.54) in *cis*-hexatriene. The calculated absorption spectra agree quite well with the experimental spectra provided a larger line width is taken for the cis isomer (70 vs 130 cm^{-1}). It is also shown that there is no mixing between the ν_5 and ν_{13} or ν_{12} modes upon electronic excitation in either of the isomers, contrary to the model presented in ref 210. It is argued that the difference of the band widths between the two isomers results from a much lower (ca. 1 kcal/mol) energy barrier for the $C_3=C_4$ torsional potential in the excited state. Such a low barrier leads to destabilization of the planar structure of the cis isomer in the $1B_1$ state thereby inducing Franck–Condon activity of low frequency ν_{19} (a_2, 160 cm^{-1}) and ν_{24} (b_2, 134 cm^{-1}) modes.

Careful resonance Raman studies of *trans*-hexatriene in the vapor phase and in different solvents in the region of the $1A_g \rightarrow 1B_u$ transition have been reported in refs 211 and 212. The analysis of excitation profiles of a_g fundamentals and overtones of the C=C torsional mode furnished "experimental" displacement parameters for the ν_5 and ν_9 modes (ν_9 mode is attributed there to ν_{10}) of 1.32 and 0.82, respectively, in good agreement with the calculated values.[85] Also the observed mixing of ν_5, ν_9 modes upon excitation to the $1B_u$ state agrees reasonably well with that resulting from theoretical calculations. It was observed that the intensities of the ν_{18} torsional overtones (first and third) dramatically decrease upon solvation. This was taken as an indication that the excited-state potential for the torsion around the central C=C bond becomes stiffer in the solvent as compared to the vapor phase.

The location of the $2A_g$ state of *trans*-hexatriene and of the $2A_1$ state of *cis*-hexatriene was unknown until very recently. It has been located by mass selectively detected multiphoton ionization of hexatriene seeded in a supersonic helium expansion beam.[59] These measurements put the origin of the $2A_1$ state of the cis isomer ca. 5270 cm^{-1} below the origin of the $1B_1$ state. For the trans isomer the corresponding energy gap is estimated to be at least 5748 cm^{-1}.

The location of the two lowest triplet states of hexatriene was established by means of electron-impact spectroscopy. The vertical gap between the ground state and the lowest triplet (1^3B_u) is 2.6 eV.[75] Its vibrational structure was not studied since the electron-impact spectrum has very low resolution. The vertical gap between the ground state and the second triplet (1^3A_g) is 4.1 eV; the spectrum is very broad with unresolved vibrational structure. It may overlap the $1A_g \rightarrow 2A_g$ transition whose origin is around 4.5 eV.[59]

9.3. Octatetraene

Octatetraene is the shortest polyene for which the $1A_g \rightarrow 2A_g$ transition can be clearly seen in one- and two-photon absorption spectra.[40,46] The one-photon absorption spectrum shows this transition in the form of four very weak false origins presumably induced by vibronic coupling between the $2A_g$ and $1B_u$ states by modes of b_u symmetry. The false origins are followed by Franck–Condon progressions of the C=C and C—C stretching modes. The distribution of intensities in the progressions is unusual in a sense that the intensity increases monotonically until the threshold of the strong $1A_g \rightarrow 1B_u$ transition is reached. This distribution probably arises from very different geometries of the borrowing and lending electronic states (non-Condon effect), as is in the case of the $A \rightarrow X$ transition in sulfur dioxide.[213] A similar situation occurs in 1,8-diphenyl-1,3,5,7-octatetraene.[125,149] Here the displacement parameters for the $1A_g \rightarrow 2A_g$ transition are 2.1 and 1.54 for the C=C and C—C stretch, respectively. The same parameters for the intense $1A_g \rightarrow 1B_u$ transition are 1.25 and 1.04,[149] so the Stokes' shift for the $2A_g$ state is twice as large as that for the $1B_u$ state leading to a conical intersection between the potential surfaces of the two states. The two-photon absorption spectrum places the origin of the $2A_g$ state at 28 561 cm^{-1}. The Franck–Condon progressions of the C=C and C—C stretching modes show a normal Poisson-type intensity distribution as expected for an allowed transition. The spectrum indicates a large increase in frequency of the C=C mode upon excitation to the $2A_g$ state (from 1612 to 1754 cm^{-1} [53]). This increase results from strong vibronic coupling between the $1A_g$ and $2A_g$ states by this mode.[88,89,137] A similar, but slightly smaller, increase in frequency occurs for the C–C mode (from 1185 to 1271 cm^{-1} [53]).

Octatetraene is the shortest unsubstituted polyene that exhibits emission. The emission spectrum corresponding to the $2A_g \rightarrow 1A_g$ transition is a good mirror image of the two-photon absorption.[1]

The intense one-photon absorption belonging to the $1A_g \rightarrow 1B_u$ transition was studied in some detail in refs 53 and 214. Again the C=C and C—C stretches (1645 and 1235 cm^{-1}) form the Franck–Condon structure of the transition. The observed progressions are much shorter than those in the $1A_g \rightarrow 2A_g$ transition, indicating smaller bond length changes upon excitation to the $1B_u$ state. The jet absorption spectrum shows a

very small line width for all bands (30–40 cm^{-1}). This is more than an order of magnitude smaller than the corresponding line width in the spectrum of butadiene. The narrower bands in the octatetraene spectrum indicate much slower radiationless decay of the $1B_u$ state into the $2A_g$ state than in butadiene. The slow decay is probably due to the planarity of the $2A_g$ state of octatetraene as opposed to butadiene,[38,39] which prevents out-of-plane modes from acting as efficient accepting modes.

The $1A_g \rightarrow 1B_u$ transition in *trans,trans*-octatetraene was analyzed theoretically.[81] The geometry of the two states involved in the transition and the corresponding force fields were calculated by the QCFF/PI method.[16] Together with the calculated displacement parameters and mode mixing matrices, they yielded good agreement with the observed spectra. For the active a_g stretches excited state frequencies of 1562 and 1184 cm^{-1} were calculated with displacement parameters of 1.22 and 1.02, respectively. Excitation leads to strong mixing of modes ν_6 and ν_7 (calculated ground state frequencies: 1614 and 1600 cm^{-1}, respectively), and also modes ν_{12} and ν_{13} (1188 and 1181 cm^{-1}). The lowest frequency skeletal bending mode ν_{17} is predicted to be the third mode active in the transition, in agreement with experiment, although its activity is underestimated by the calculations.

The absorption spectrum of *cis,trans*-octatetraene,[215] corresponding to the counterpart of the $1A_g \rightarrow 1B_u$ transition of the all trans isomer, seems to indicate a larger line width than the spectrum of the trans,trans isomer. This effect would be similar to that reported for hexatriene. It is argued[206] that the cis linkage increases the number of Franck–Condon-active totally symmetric modes in the transition.

9.4. Longer Polyenes

Absorption spectra of decapentaene and dodecahexaene corresponding to the $1A_g \rightarrow 1B_u$ transition were reported in ref 45. They indicate similar activity of the a_g modes as in the shorter polyenes. Thus the C=C and C—C stretches dominate the transition, the former being the most active modes. Fluorescence excitation spectra of dodecapentaene taken at 4.2 K in undecane matrix[1] locate the origin of the $2A_g$ state 0.42 eV below the origin of the $1B_u$ state. They confirm that there is a large increase of the active C=C stretch mode frequency upon excitation to the $2A_g$ state. The vibrational structure of the $1A_g \leftarrow 1B_u$ fluorescence excitation spectrum differs from the structure of the corresponding absorption spectrum, indicating a large dependence of the radiationless decay rate constant of the $1B_u$ state on the excess of energy put into its vibrational manifold.

Fluorescence and fluorescence excitation spectra of a Schiff base—a derivative of dodecapentaene (five C=C bonds and one C=N bond), measured at liquid helium temperature in *n*-tetradecane matrix,[47] allows a detailed study of the vibrational structure of the $1A_g \leftrightarrow 2A_g$ transitions. These spectra show no frequency increase of the Franck–Condon-active C=C stretch mode upon electronic excitation, but instead a decrease from 1589 cm^{-1} in the $1A_g$ state to 1544 cm^{-1} in the $2A_g$ state. In the closely related tetradecahexaene molecule, the corresponding frequencies are 1576 and 1779 cm^{-1}, respectively.[42] Apparently a substitution of a terminal CH_2 group by a butyl amine group causes a 250 cm^{-1} decrease of the C=C stretch frequency in the lowest excited singlet state. A similar effect occurs in dodecapentaenal, an analogue of retinal,[126] where the excited-state frequency of this mode is only 1636 cm^{-1}. This difference between unsubstituted and substituted polyenes was explained in terms of symmetry lowering that permits the totally symmetric C=C stretch to couple the S_1 and S_2 states.[140] The calculated S_1–S_2 vibronic coupling strengths via the C=C stretch in the Schiff base and dodecapentaneal[140] fully explain the lowering of the C=C stretch frequency in the S_1 state of these molecules as compared to the frequency of an unsubstituted polyene.

The absorption spectrum of retinal differs dramatically from the spectra of polyenes of equal length by the very large band width of its vibronic lines, such that individual vibrational lines cannot be resolved, their width being at least 1000 cm^{-1}.[216,217] It was shown empirically that the large width is caused by the presence of the cyclohexene ring.[218] Theoretical calculations suggest that the very low potential barrier in the electronic ground state for twisting around the CC bond that links the polyene chain to the cyclohexene ring, becomes quite large upon HOMO → LUMO excitation.[219,220] Thus the electronic transition should involve very strong Franck–Condon activity of a low-frequency mode describing torsion around this CC bond. Indeed, saturation of the cyclohexene double bond eliminates the broadening effect of the torsion around the C_6–C_7 bond; the potentials for this torsion are the same in the ground and excited states as there is no π-electron coupling with the ring.[221] Therefore 5,6-dihydro-*all-trans*-retinal shows a sharp absorption spectrum in which main vibronic bands can be separated while its resonance Raman spectrum shows almost the same relative activity of various totally symmetric modes as retinal. It is interesting to note that the Franck–Condon activity that was concentrated in the C–C stretch in unsubstituted polyenes is distributed in retinal over several modes with frequencies in the range of 950–1350 cm^{-1}. The Franck–Condon activity of the C=C stretch remains localized, however. The resonance Raman studies indicate that the broadening of the retinal spectrum is purely homogeneous and arises from long Franck–Condon progressions of the low frequency torsion about the C_6–C_7 bond.[221] Raman bands associated with this torsion appear at 194, 306, and 480 cm^{-1}.

The absorption spectrum of β-carotene is dominated by three totally symmetric modes: a C=C stretch mode with a ground-state frequency of 1525 cm^{-1}, a C—C stretch mode (1155 cm^{-1}), and a C—CH_3 stretch mode (1005 cm^{-1}).[222] Analysis of the resonance Raman excitation profiles of the fundamentals, overtones and combination bands of these modes leads to displacement parameters of these modes for the $1A_g \rightarrow 1B_u$ transition of 1.06, 0.93 and 0.56 for the C=C, C—C, and C—CH_3 stretches, respectively.[223] It is interesting to note that the displacement for the C=C stretch is smaller in β-carotene than for shorter polyenes.

Nystatin provides an example of a polyene derivative that is composed of two interacting conjugated π-electron chains: a diene and a tetraene. It has been shown[150] that this interaction leads to Franck–Condon activity of the out-of-phase a_g stretch in the transition

to the lowest excited state which is dominated by the HOMO → LUMO excitation on the tetraene unit. Thus the resonance Raman spectrum of nystatin shows two tetraenic fundamentals in the C=C stretch region,[224] one being the highest frequency in-phase stretch, active in all polyenes, the second other being the lower frequency out-of-phase stretch.[150] The interaction between these two modes via the diene unit leads to an increase in frequency of the strongly active in-phase C=C stretching mode.

Transient resonance Raman spectra from the $2A_g$ state of β-carotene in the region of the $S_1 \rightarrow S_n$ transition were recorded recently by two independent groups.[127,225] They indicate strong activity of the CC double and single bond stretches in this transition. The C=C bond stretch frequency in the S_1 state was found to be 1777 cm^{-1} in *all-trans*-β-carotene and 1760 cm^{-1} in its 15-cis isomer. The C–C bond stretch in the S_1 state was found to be spread over three different modes with frequencies of 1204, 1243, and 1282 cm^{-1}; the mode of intermediate frequency seems to possess most of the C–C stretch character. The increase of the C=C stretch frequency in the S_1 state of β-carotene indicates its involvement in strong S_0–S_1 vibronic coupling.

9.5. Polyacetylene

The electrical properties of doped and/or photoexcited polyacetylenes, the nature of their excited states as seen by solid-state physics and their insulator to metal transition were discussed recently in very good reviews.[226,227] In this subsection we review only the authors' contribution to the field.

The absorption spectrum of polyacetylene is characterized by a very broad band showing little structure. The spectrum of the soluble trans isomer is especially broad, showing only traces of the underlying vibrational structure. A shoulder that can be ascribed to origin to the $1B_u$ state is located at ca. 15900 cm^{-1}.[228] The spectrum itself depends on the way the sample was prepared. The spectrum of the cis isomer is sharper and more structured. The peak that belongs to the origin of the $1B_1$ singly excited state is located at ca. 16700 cm^{-1}. Its prominence varies among different samples.[229] The large width of the absorption spectra is attributed mainly to inhomogeneous broadening since the two polymers are mixtures of molecules of different length of the polyene chain. Hence the absorption spectra are not very useful as a source of information on the excited states of these polymers.

More informative are resonance Raman excitation profiles of the totally symmetric modes, which show that there is an interesting difference in the Franck–Condon activity of the totally symmetric modes in the two isomers and their deuterated isotopomers. Thus, while cis-$(CH)_x$ and trans-$(CD)_x$ have three Franck–Condon-active modes of 1540, 1250, 910 cm^{-1} and 1330, 1200, 840 cm^{-1}, respectively,[229,230] there are only two Franck–Condon-active modes in the trans-$(CH)_x$ and cis-$(CD)_x$, namely 1456, 1064 cm^{-1} and 1470, 976 cm^{-1}, respectively.[229,231,232]

The excitation profiles of the fundamentals, overtones, and combination bands of the two cis isotopomers were investigated theoretically to extract the displacement parameters and distribution of chain lengths in the polymer.[233,234] It was concluded that the displacement parameters of the three active modes in the cis-$(CH)_x$ polymer are somewhat smaller than those in β-carotene. The distribution of chain lengths was found to be fairly sharp and to peak at about 18 C=C bonds. Analysis of the excitation profiles of the trans-$(CH)_x$ led to similar values of the displacement parameters for the active totally symmetric modes.[228]

Theoretical calculation of the displacement parameters for the $1A_g \rightarrow 1B_u$ and $1A_1 \rightarrow 1B_1$ transition in the *all-trans*- and *all-cis*-polyenes, respectively, properly reproduces the observed numbers of the Franck–Concon-active modes as a function of the chain length.[18] Thus for the $C_{36}H_{38}$ polyene, it gives the following frequencies (displacement parameters): 1604 (1.27), 1164 cm^{-1} (1.19) for the trans isomer, and 1590 (1.3), 1287 (0.89), 943 cm^{-1} (0.7) for the cis isomer. The corresponding numbers for the fully deuterated isotopomers read 1545 (1.45), 1284 (0.6), 872 cm^{-1} (0.81) for the trans isomer and 1549 (1.45), 1003 cm^{-1} (0.84) for the cis isomer.

Measurements of the depolarization ratios of the fundamentals of the totally symmetric modes corresponding to the C=C and C—C stretches indicate that two electronic states of perpendicular polarization contribute to the observed absorption spectrum of soluble *trans*-polyacetylene.[235] The second transition may belong to the forbidden A_g state which becomes allowed due to a number of accidental cis linkages in the trans polymer as observed in the absorption spectrum of 15-*cis*-β-carotene.[236]

10. Radiationless Decay in Polyenes

Polyenes show an interesting radiationless decay pattern. The two shortest polyenes, butadiene and hexatriene, exhibit no known fluorescence which indicates that radiationless decay of the lowest excited singlet is very fast. The next polyene, octatetraene, shows however, the largest fluorescence quantum yield among all polyenes. In longer polyenes this yield decreases monotonically with increasing length of the polyene chain[7,148] and approaches zero in *trans*-polyacetylene where again no fluorescence is observed. Since, in most cases, fluorescence originates from the $2A_g$ state (exceptions are, however, reported in ref 237 for long polyenes), its quantum yield reflects the rate of radiationless decay of this state. If there is fluorescence only from the $2A_g$ state, the decrease of this yield with increasing chain length can be qualitatively understood in terms of the energy-gap law, since the longer the polyene the smaller is the excitation energy for the $1A_g \rightarrow 2A_g$ transition. The large decay rate in butadiene and hexatriene runs counter to the energy-gap law, since their excitation energies are the largest among polyenes.

It has been shown by ab initio force field calculations that the equilibrium configuration of the $2A_g$ state is nonplanar in butadiene and hexatriene in contrast to the configuration of the same state in other polyenes.[38,39] This, coupled with the planar conformation of the ground state, makes out-of-plane vibrations effective accepting modes in the process of internal conversion. Substitution of terminal hydrogen atoms with some heavy substituents can influence the out-of-plane deformation of butadiene changing drastically the decay rate. Thus 1,4-diphenylbutadiene exhibits very strong fluorescence with a quantum yield much larger than

TABLE 22. Calculated Relative Rate Constants for the Internal Conversion $2A_g \rightarrow 1A_g$ in Polyenes (after ref 38)

model molecule	relative rate constant[a]	model molecule	relative rate constant[a]
C_4, planar	$1.57 \cdot 10^{-3}$	C_{10}, planar	$1.94 \cdot 10^{0}$
C_4, twisted 38° [b]	$6.67 \cdot 10^{2}$	C_{12}, planar	$1.18 \cdot 10^{1}$
C_4, twisted 45° [a]	$2.94 \cdot 10^{4}$	C_{14}, planar	$2.67 \cdot 10^{1}$
C_8, planar	$1.00 \cdot 10^{0}$	C_{14}, planar[c]	$6.57 \cdot 10^{1}$

[a] Relative to the calculated rate for planar C_8. [b] About one of C=C bonds. [c] Lower torsional frequency and barrier (see text).

that of octatetraene,[238] in accordance with the energy-gap law. Since the decaying states in butadiene and in 1,4-diphenylbutadiene are similar, only a drastic change in configuration of that state upon substitution of hydrogen atoms with phenyl groups can be responsible for a dramatic reduction of the radiationless decay rate constant. A similar situation occurs in 1,6-diphenylhexatriene.[1,238,239]

The radiationless decay of the $2A_g$ state can occur by internal conversion to the ground state or by intersystem crossing to $^3 1B_u$ or $^3 1A_g$ state. The absence of an external heavy atom effect on the fluorescence quenching in polyenes[240] suggests that the intersystem crossing plays a minor role in the decay of the $2A_g$ state which must therefore proceed through the $2A_g \rightarrow 1A_g$ channel. This conclusion is further supported by the absence of phosphorescence in all polyenes.

Quantum chemical calculations identify the highest frequency C=C stretching mode of a_g symmetry as the effective promoting mode for the $2A_g \rightarrow 1A_g$ internal conversion.[87,88,137,140,207] This mode shows also the strongest Franck–Condon activity in $1A_g \leftrightarrow 2A_g$ transitions,[38,88,140,149] so that it can act as an effective accepting mode. Since both its frequency and displacement parameter are much larger than those of the Franck–Condon-active mode in the $S_0 \rightarrow S_1$ transition in benzene and other aromatic hydrocarbons (1600 vs 990 cm^{-1} and 2.5 vs 1.45[38,241], it can compete with local C–H stretching vibrations in accepting the electronic energy released in the internal conversion. Indeed, recent measurements[242] indicate that full deuteration of β-carotene changes the lifetime of its excited state only slightly, indicating that C–H stretching modes play a minor role in the radiationless decay in polyenes, in contrast to their dominant role in planar aromatic molecules.[241,243–245]

To understand the radiationless decay pattern seen in polyenes, at least two (effective modes) are needed,[38] namely the Franck–Condon-active C=C stretching vibration and an out-of-plane torsion. The C=C stretch acts both as promoting and accepting mode. It dominates the radiationless decay in polyenes with a planar configuration of the S_1 state. The torsion can act as an accepting mode in the decay of the S_1 state with a strongly out-of-plane distorted configuration, as in the case of butadiene and hexatriene. The participation of this out-of-plane mode increases the rate of internal conversion by several orders of magnitude, as shown in Table 22 where the calculated rate constants of the decay of a planar and twisted $2A_g$ state of butadiene are given. This model[38] predicts that up to 50% of the electronic energy is taken by out-of-plane torsional a_u and b_g modes in the internal conversion process in *s-trans*-butadiene. The situation is somewhat similar to that occurring in the intersystem crossing governing the decay of the T_1 state in benzene, where also a nontotally symmetric vibration accepts a large amount of the electronic energy.[246,247] However, while in butadiene this results from a large geometry distortion upon excitation, in benzene it results from vibronic coupling between the T_1 and T_2 states.

According to the calculations, the rate constant of internal conversion in the twisted butadiene molecule greatly exceeds that in planar octatetraene. Two values of the rate constant for twisted butadiene are listed in Table 22, the lower value refers to a rotation by ca. 38° about the terminal $=CH_2$ bond, while the larger value corresponds to a rotation by 45°. Thus the calculations indicate that the ultrafast decay of the excited-singlet state of butadiene and hexatriene results from the participation of the out-of-plane torsional modes in the process. For longer polyenes the model reproduces the observed increase in the decay with increasing chain length. This is mostly due to the decrease in the energy gap with increasing chain length. The corresponding increase of the Franck–Condon overlap factor that governs the internal conversion is moderated to some extent by a slight decrease of the displacement parameter of the promoting C=C stretch vibration.[88,140] In addition, there is a corresponding decrease in torsional frequencies and barriers, reflecting the increased flexibility of longer polyenes. The resulting effect is illustrated in Table 22 for tetradecaheptaene (last entry in the second column) where the barrier for the torsion was lowered by a factor of 5 and the torsional frequency was lowered by a factor of 4 with respect to the other entry for this molecule. However, such drastic changes of the torsional modes characteristics in a planar polyene cause only modest changes in the rate of internal conversion (65.7 vs 26.7).

We have thus a reasonably good understanding of the radiationless decay of optically excited polyenes. Absorption of a photon puts the molecule into the second excited singlet of the $1B_u$ symmetry. The conformation of this state is planar[209] or nearly planar.[80] It undergoes very rapid internal conversion to the $2A_g$ manifold of which the zero-point level is separated from the origin of the $1B_u$ state by only 2000–4000 cm^{-1}. This transition is facilitated by b_u modes[140,248] and by the conical intersection of the $1B_u$ and $2A_g$ state potential surfaces.[149] Although the minimum of the potential is lower in the $2A_g$ state, the $1B_u$ state potential surface has the lower energy for the ground-state configuration. The $2A_g$ state then decays to the $1A_g$ state either by fluorescence or by internal conversion. Population of the 1^3B_u and 1^3A_g states by intersystem crossing is very inefficient. Internal conversion is much faster than radiative decay in butadiene, hexatriene, and very long polyenes. In the first two, S_1 is nonplanar, so that out-of-plane b_g and a_u modes become efficient accepting modes. In longer polyenes, the small energy gap is the main cause of the rapid internal conversion, although out-of-plane accepting modes contribute significantly for long and hence flexible molecules.

11. Conclusions

The ground state properties of polyenes with less than 20 carbon atoms are now under reach of accurate theoretical calculations and are essentially well-understood. In particular, the alternancy of the CC bond

length has been shown to hold even for long polyenes. Theoretical force fields lead to reliable assignments of vibrational IR and Raman spectra. The anomalously low frequency of the Franck–Condon-active C=C stretch mode in the S_0 state has been attributed to the geometry-dependent interaction between the $1A_g$ and $2A_g$ states, i.e., it is caused by an adiabatic or Herzberg–Teller coupling. The dependence of the CC stretch vibrational frequency on the length of polyene chain is rationalized in terms of this vibronic coupling. The same coupling explains the anomalous increase of the frequency of the same mode upon $1A_g \rightarrow 2A_g$ excitation.

The ordering of the lowest singlet electronic states is now firmly established. Semiempirical calculations and spectroscopic observations have pointed out long ago that the lowest excited state in octatetraene and longer polyenes is of A_g symmetry. Recently, accurate quantum chemical calculations and supersonic beam multiphoton ionization experiments have shown that the same conclusion applies also to the shorter polyenes.

The characterization of the properties of the potential energy surfaces of the lowest excited states has been actively pursued both theoretically and experimentally. The lowest singlet states have been explored mainly by absorption, emission, and resonance Raman spectroscopy, while the lowest triplet state has been investigated mainly by transient resonance Raman spectroscopy. The shorter polyenes, like butadiene and hexatriene, have been studied by sophisticated ab initio methods, while longer polyenes have been analyzed by semiempirical methods. A reasonably accurate description of vibrational force fields in the excited states is being provided. A convincing picture of the mechanism of radiationless transitions in the short and long polyenes begins to emerge. Thus, the short lifetime of the S_1 state in butadiene and hexatriene is related to their nonplanar equilibrium geometry, while it is due to a small S_0–S_1 energy gap in long polyenes.

As for the future, the study of excited-states properties will be the main objective. We need to learn more about potential energy surfaces in the lowest excited states, their conical intersections, and their interactions to get a detailed picture of photophysical properties of polyenes. This will form a basis for a deeper understanding of their more interesting properties like photoconductivity in long polyenes, which are building blocks of polyacetylene and at the same time are related to the biologically interesting molecules like carotene and retinal.

12. Appendix A. Adiabatic Vibronic Couplings

In this appendix, we briefly review one of the possible approaches to the calculation of adiabatic vibronic coupling integrals.[139] This numerical method employs a floating orbital scheme together with a molecular Hamiltonian of the ZDO (zero differential overlap) type, namely CNDO/S (complete neglect of differential overlap/spectroscopic parametrization).[138] The floating orbital scheme introduces straightforwardly the diabaticity because the molecular orbitals and the configuration interaction coefficients remain frozen along the normal coordinate, thus obeying the definition of diabaticity. Hence any changes in the potential energy surface with respect to the nuclear coordinates are due solely to changed values of the electronic integrals. The ZDO approximation amounts to the assumption that the atomic orbital overlap matrix is diagonal. This, in turn, avoids the nonorthogonality which would arise if, along the normal coordinate, coefficients were used that are calculated at a different geometry.

The calculation proceeds as follows:

1. The reference geometry Q_0 is chosen and the molecular orbitals and the configuration interaction coefficients C's are calculated and stored for future use; this is the zero-order calculation.
2. The new geometry $Q_0 + \Delta Q$ is generated and a new CI matrix **A** is calculated with the atomic integrals of this new structure and the previously calculated molecular orbitals.
3. Finally, the **A** matrix is transformed into the basis of the CI coefficients of the reference structure through a rotation: the off-diagonal elements are proportional to the vibronic coupling integrals.

13. Appendix B. Dushinsky Effect Induced by Vibronic Coupling

Let us consider a model system with two electronic diabatic states, i and j, and with two vibrational modes, Q_a and Q_b. The potential energy surfaces of these states read:

$$E_k(Q_a,Q_b) = E_k^0 + 0.5(\Omega_{0,a}^2 Q_a^2 + \Omega_{0,b}^2 Q_b^2) \quad (8)$$

where a, b are two vibrational modes assumed to be harmonic, and the same convention used before holds for the remaining symbols. Notice that for simplicity, no displacement is assumed. Limiting the vibronic perturbation to linear terms gives

$$U_{ij} = V_{ij}^a Q_a + V_{ij}^b Q_b \quad (9)$$

The adiabatic potential energy surfaces read

$$E_i^{ad}(Q_a,Q_b) = E_i^0 + 0.5(\omega_{i,a}^2 Q_a^2 + \omega_{i,b}^2 Q_b^2) + f_{ij} Q_a Q_b \quad (10)$$

$$E_j^{ad}(Q_a,Q_b) = E_j^0 + 0.5(\omega_{j,a}^2 Q_a^2 + \omega_{j,b}^2 Q_b^2) - f_{ij} Q_a Q_b \quad (11)$$

where

$$f_{ij} = 2E_0^{-1}(\Omega_{0,a}\Omega_{0,b})^{1/2} V_{ij}^a V_{ij}^b \quad (12)$$

After the introduction of the coupling, the modes are no longer orthogonal, i.e., they are no longer normal and do not diagonalize the adiabatic force field matrix (this is hardly a surprise since we have added some terms to the molecular Hamiltonian). To regain orthonormality, the modes must be rotated by an angle which is function of the couplings through f_{ij}.

Writing explicitly for the ith state, we get

$$\begin{vmatrix} Q_{i,a}^{ad} \\ Q_{i,b}^{ad} \end{vmatrix} = \mathbf{J}_i^{ad} \cdot \begin{vmatrix} Q_a \\ Q_b \end{vmatrix} \quad (13)$$

where

$$\mathbf{J}_i^{ad} = \begin{vmatrix} \cos\phi & \sin\phi \\ -\sin\phi & \cos\phi \end{vmatrix} \quad (14)$$

and

$$\tan 2\phi = \frac{2f_{ij}}{(\omega_{i,a}^2 - \omega_{i,b}^2)} \quad (15)$$

Equations for the jth state are identical with i replaced by j. The normal mode rotation induced by the

coupling also affects the vibrational frequencies, although usually to much less an extent than the direct mechanism shown before; the new frequencies are given by

$$\bar{\omega}_{i,a} = (\omega_{i,a}^2 + f_{ij} \tan \phi)^{1/2} \quad (16)$$

$$\bar{\omega}_{i,b} = (\omega_{i,b}^2 - f_{ij} \tan \phi)^{1/2} \quad (17)$$

where $\omega_{i,a} > \omega_{i,b}$ was assumed.

Thus in the two-mode, two-state model the combined action of the two couplings also rotates the vibrational modes and adds a further shifts to the frequencies. Notice that the angle of rotation has a different sign in the lower and the upper state, but the frequency shift added by the combination of the two couplings is the same in the two states.

14. Appendix C. Diabatic Structures and Force Fields

The QCFF/PI model[16,17] employs an empirical potential for the σ-electron framework and a semiempirical quantum chemical calculation for the π-electrons, which consists of a self-consistent field (SCF) calculation followed by configuration interaction (CI). In the following, we show how to calculate diabatic gradients and Hessians for any multiplicity and any order of excitation.

First, we express the total energy as a sum

$$E = E(\mathrm{SCF}) + \Delta V \quad (18)$$

The SCF energy with respect to the nuclear coordinates has been derived a number of times, and we shall not dwell upon it. Notice that from the definition of self-consistency, the SCF energy gradient is both diabatic and adiabatic. This does not hold true for the SCF Hessian. To derive the CI contribution to the energy, we must express ΔV as a function of the one-electron integrals, α,β, the two-electron integrals, γ, and certain electron density coefficients, R, which contain the CI coefficients C and the molecular orbitals υ.

$$\Delta V = \sum_{\nu}(R_{\nu}^{\alpha}\alpha_{\nu} + R_{\nu}^{\gamma}\gamma_{\nu}) + \sum_{\mu\neq\nu}(R_{\nu\mu}^{\beta}\beta_{\nu\mu} + R_{\nu\mu}^{\gamma}\gamma_{\nu\mu}) \quad (19)$$

In the adiabatic representation, both R and the electronic integrals depend on nuclear coordinates. In the diabatic picture, R is kept constant at the equilibrium values which are obtainable through minor manipulation. To this end, we write

$$\Delta V = \sum_{m,k} C_{N,m} A_{m,k} C_{k,N} \quad (20)$$

where the sum runs over all electronic configurations. As usual Latin letters refer to molecular and Greek letters to atomic quantities. The CI matrix elements A_{mk} are expressed in terms of Hartree–Fock matrix elements F_{mn} and two-electron integrals $\langle mn|kl\rangle$ in the molecular basis:

$$F_{mn} = \sum_{\nu,\mu} \upsilon_{m\nu} F_{\nu\mu} \upsilon_{n\mu} \quad (21)$$

$$\langle nm|kl\rangle = \sum_{\nu,\mu} \upsilon_{n\mu}\upsilon_{k\mu}\upsilon_{m\nu}\upsilon_{l\nu}\gamma_{\nu\mu} \quad (22)$$

where, for the QCFF/PI Hamiltonian,

$$F_{\mu\mu} = \alpha_{\mu} + 0.5\gamma_{\mu\mu}P_{\mu\mu} - \sum_{\nu\neq\mu}\gamma_{\nu\mu}Q_{\nu} \quad (23)$$

$$F_{\mu\nu} = \beta_{\mu\nu} - 0.5P_{\mu\nu}\gamma_{\mu\nu} \quad (24)$$

and

$$P_{\mu\nu} = 2\sum_{n} \upsilon_{n\mu}\upsilon_{n\nu} \quad (25)$$

$$Q_{\nu} = Z_{\nu} - P_{\nu\nu} \quad (26)$$

Z_{ν} being the number of π-electrons on the νth atom. The contributions to the R from the F are now given by

$$R_{\nu}^{\alpha} = \sum_{m} C_{N,m}^2 \sum_{n_1,n_2}^{(m)} \upsilon_{n_1,\nu}\upsilon_{n_2,\nu} + 2\sum_{m}\sum_{k>m} C_{N,m}C_{N,k} \sum_{n_1,n_2}^{(m,k)} \upsilon_{n_1,\nu}\upsilon_{n_2,\nu} \quad (27)$$

$$R_{\nu}^{\gamma} = 0.5R_{\nu}^{\alpha}P_{\nu\nu} \quad (28)$$

$$R_{\mu\nu}^{\beta} = \sum_{m} C_{N,m}^2 \sum_{n_1,n_2}^{(m)} (\upsilon_{n_1,\nu}\upsilon_{n_2,\mu} + \upsilon_{n_1,\mu}\upsilon_{n_2,\nu}) + 2\sum_{m}\sum_{k>m} C_{N,m}C_{N,k} \sum_{n_1,n_2}^{(m,k)} (\upsilon_{n_1,\nu}\upsilon_{n_2,\mu} + \upsilon_{n_1,\mu}\upsilon_{n_2,\nu}) \quad (29)$$

$$R_{\mu\nu}^{\gamma} = -\sum_{m} C_{N,m}^2 \sum_{n_1,n_2}^{(m)} [\upsilon_{n_1,\nu}\upsilon_{n_2,\nu}Q_{\mu} + \upsilon_{n_1,\mu}\upsilon_{n_2,\mu}Q_{\nu} + 0.5P_{\mu\nu}(\upsilon_{n_1,\nu}\upsilon_{n_1,\mu} + \upsilon_{n_2,\nu}\upsilon_{n_2,\mu})] - 2\sum_{m}\sum_{k>m} C_{N,m}C_{N,k} \sum_{n_1,n_2}^{(m,k)} [\upsilon_{n_1,\nu}\upsilon_{n_2,\nu}Q_{\mu} + \upsilon_{n_1,\mu}\upsilon_{n_2,\mu}Q_{\nu} + 0.5P_{\mu\nu}(\upsilon_{n_1,\nu}\upsilon_{n_2,\mu} + \upsilon_{n_1,\mu}\upsilon_{n_2,\nu})] \quad (30)$$

where the summation indices n_1, n_2 run over all combinations of molecular orbitals involved in the configurations indicated in parentheses above the summation sign.

The two-electron integrals contribute only to R_{ν}^{γ} and $R_{\mu\nu}^{\gamma}$. These contributions are

$$R_{\mu\nu}^{\gamma} = \sum_{m} C_{N,m}^2 \sum_{n_1,l_1,n_2,l_2}^{(m)} (\upsilon_{n_1,\nu}\upsilon_{l_1,\nu}\upsilon_{n_2,\mu}\upsilon_{l_2,\mu} + \upsilon_{n_1,\mu}\upsilon_{l_1,\mu}\upsilon_{n_2,\nu}\upsilon_{l_2,\nu}) + 2\sum_{m}\sum_{k>m} C_{N,m}C_{N,k} \sum_{n_1,l_1,n_2,l_2}^{(m,k)} (\upsilon_{n_1,\nu}\upsilon_{l_1,\nu}\upsilon_{n_2,\mu}\upsilon_{l_2,\mu} + \upsilon_{n_1,\mu}\upsilon_{l_1,\mu}\upsilon_{n_2,\nu}\upsilon_{l_2,\nu}) \quad (31)$$

$$R_{\nu}^{\gamma} = \sum_{m} C_{N,m}^2 \sum_{n_1,l_1,n_2,l_2}^{(m)} \upsilon_{n_1,\nu}\upsilon_{l_1,\nu}\upsilon_{n_2,\nu}\upsilon_{l_2,\nu} + 2\sum_{m}\sum_{k>m} C_{N,m}C_{N,k} \sum_{n_1,l_1,n_2,l_2}^{(m,k)} \upsilon_{n_1,\nu}\upsilon_{l_1,\nu}\upsilon_{n_2,\nu}\upsilon_{l_2,\nu} \quad (32)$$

Implementation of these equations to calculate the atomic coefficients R is straightforward and has been presented before.[87,249]

15. Appendix D. Displacement Parameters and Dushinsky Matrices

The Franck–Condon activity of the ith mode is governed by its γ-parameter which corresponds to one-half of the Stokes shift. For the electronic transition from the nth electronic state to the mth electronic state, this γ-parameter is given by

$$\gamma_i^{nm} = 0.5B_{i,nm}^2 \quad (33)$$

where $B_{i,nm}$ is the projection along the ith normal coordinate expressed in dimensionless units as the dif-

ference between the equilibrium geometries of the two states ($\mathbf{X}_m - \mathbf{X}_n$):

$$B_{i,nm} = 0.172\omega_i^{1/2}[(\mathbf{X}_m - \mathbf{X}_n)\mu^{1/2}\mathbf{L}_n]_i \quad (34)$$

Here ω_i is the vibrational frequency, μ is the $3N \times 3N$ diagonal matrix of the atomic masses expressed in atomic units, and $\mathbf{L}_n$ is the vector describing the ith normal mode in the nth electronic state. In the absence of normal-mode rotation (Dushinsky effect), these expressions are exact in the harmonic approximation.

The calculation of the rotation matrix between normal modes is easily accomplished by overlapping the normal-mode matrices $\mathbf{L}_m$ and $\mathbf{L}_n$, of the two states involved in the electronic transition

$$J_{ij}^{mn} = \sum_{k}^{[3N]} L_{ik,m}L_{kj,n} \quad (35)$$

where N is the number of atoms. Notice that this **J** matrix is not the same of that in Appendix B. Both represent normal mode rotation, and both are called **J**. The matrix introduced above directly enters in the Franck–Condon integrals calculation, as described in ref 250.

16. Appendix E. Rotation of the Force Field Matrix

Quantum chemical calculations are usually performed in Cartesian coordinates. It is sometimes useful to express a force field matrix in internal coordinates because this gives a more detailed understanding of frequency variations from molecule to molecule and/or state to state. The problem arises because the force field matrix in internal coordinates spans a $3N$ dimensional space, with N being the number of atoms, while the number of nonredundant internal coordinates is only $3N - 6$ (or $3N - 5$ for linear molecules). Moreover the internal coordinates are usually nonorthonormal. The transformation from Cartesian to internal coordinates can be described as follows.[251] The potential energy surface of a given state can be described both in Cartesian coordinates

$$E(\mathbf{x}) = E_0(\mathbf{x}) + \mathbf{g}\cdot\mathbf{x} + 0.5\mathbf{x}\cdot\mathbf{H}\cdot\mathbf{x} + \ldots \quad (36)$$

and in internal coordinates

$$E(\mathbf{s}) = E_0(\mathbf{s}) + \mathbf{f}\cdot\mathbf{s} + 0.5\mathbf{s}\cdot\mathbf{F}\cdot\mathbf{s} + \ldots \quad (37)$$

where $\mathbf{s} = \mathbf{B}\cdot\mathbf{x}$ is the internal coordinate vector, $\mathbf{x}$ is the Cartesian vector, $\mathbf{g}$ and $\mathbf{f}$ are gradients, $\mathbf{H}$ and $\mathbf{F}$ are the second derivative matrices in the two frameworks, and $\mathbf{B}$ is the Wilson's $\mathbf{B}$ matrix which transforms Cartesian into internal coordinates. By inspection, we find

$$\mathbf{F} = \mathbf{B}^{-1\dagger}\cdot\mathbf{H}\cdot\mathbf{B}^{-1} \quad (38)$$

Since $\mathbf{B}$ is a rectangular matrix, to invert it, it is necessary to use the notion of generalized inverse matrix:

$$\mathbf{B}^{-1\dagger} = (\mathbf{B}\cdot\mathbf{B}^{\dagger})^{-1}\cdot\mathbf{B} \quad (39)$$

Acknowledgments. G.O. is grateful to MURST and CNR for financial support.

References

(1) Hudson, B. S.; Kohler, B. E.; Schulten, K. *Excited States* **1982**, *6*, 1. Hudson, B. S.; Kohler, B. E. *Annu. Rev. Phys. Chem.* **1974**, *24*, 437.
(2) Birge, R. R. *Annu. Rev. Phys. Chem.* **1990**, *41*, 683.
(3) *Conjugated Polymeric Materials: Opportunities in Electronics, Optoelectronics and Molecular Electronics*; Bredas, J. L., Chance, R. R., Eds.; NATO ASI Series E 182; Reidel: Dordrecht, 1990.
(4) Haugen, W.; Traettenberg, M. *Acta Chem. Scand.*, **1966**, *20*, 1726. Traettenberg, M. *Acta Chem. Scand.* **1968**, *22*, 628.
(5) Traettenberg, M. *Acta Chem. Scand.* **1968**, *22*, 2294.
(6) Baughman, R. H.; Kohler, B. E.; Levy, J. J.; Spangler, C. S. *Synth. Met.* **1985**, *11*, 37.
(7) Lasaga, A. C.; Aerni, R. J.; Karplus, M. *J. Chem. Phys.* **1980**, *73*, 5230.
(8) Szalay, P. G.; Karpfen, A.; Lischka, H. *J. Chem. Phys.* **1980**, *87*, 3530.
(9) Hamilton, T. P.; Pulay, P. *J. Phys. Chem.* **1989**, *93*, 2341.
(10) Peierls, P. E. *Quantum Theory of Solids*; Clarendon: Oxford, 1955; p 108.
(11) Salem, L. *The Molecular Orbital Theory of Conjugated Systems*; Benjamin: New York, 1966.
(12) Rimai, L.; Heyde, M. E.; Gill, D. *J. Am. Chem. Soc.* **1973**, *95*, 4493.
(13) Villar, H. O.; Dupuis, M.; Watts, J. D.; Hurst, G. J. B.; Clementi, E. *J. Chem. Phys.* **1988**, *88*, 1003.
(14) Dewar, M. J. S.; Thiel, W. *J. Am. Chem. Soc.* **1977**, *99*, 4899.
(15) Boudreaux, D. S.; Chance, R. R.; Bredas, J. L.; Silbey, R. *Phys. Rev.* **1983**, *B28*, 6927.
(16) Warshel, A.; Karplus, M. *J. Am. Chem. Soc.* **1972**, *94*, 5612.
(17) Warshel, A.; Levitt, M. *QCPE* No. 247, **1974**.
(18) Zerbetto, F.; Zgierski, M. Z. *Chem. Phys. Lett.* **1988**, *143*, 153.
(19) Fincher, C. R., Jr.; Chen, C. E.; Heeger, A. J.; McDiarmid, A. G.; Hastings, J. B. *Phys. Rev. Lett.* **1982**, *48*, 100.
(20) Yannoni, C. S.; Clarke, T. C. *Phys. Rev. Lett.* **1983**, *51*, 1191.
(21) Carreira, L. A. *J. Chem. Phys.* **1975**, *62*, 3851.
(22) Bock, C. W.; George, P.; Trachtman, M.; Zanger, M. *J. Chem. Soc. Perkin Trans. 2* **1976**, 26.
(23) Fischer, J. J.; Michl, J. *J. Am. Chem. Soc.* **1987**, *109*, 1056.
(24) Arnold, B. R.; Balaji, V.; Michl, J. *J. Am. Chem. Soc.* **1990**, *112*, 1808.
(25) Alberts, I. L.; Schaefer, H. F. III *Chem. Phys. Lett.* **1989**, *161*, 375.
(26) Rice, J. E.; Liu, B.; Lee, T. J.; Rohlfing, C. M. *Chem. Phys. Lett.* **1989**, *161*, 277.
(27) Bock, C. W.; George, P.; Trachtman, G. P. *Theor. Chim. Acta* **1984**, *64*, 293.
(28) De Maré, G. R. *J. Mol. Struct.* (THEOCHEM) **1984**, *107*, 127.
(29) Wilberg, K. B.; Rosenberg, R. E. *J. Am. Chem. Soc.* **1990**, *112*, 1509.
(30) Guo, H.; Karplus, M. *J. Chem. Phys.* **1991**, *94*, 3679.
(31) Hudson, B. R.; Kohler, B. E. *Chem. Phys. Lett.* **1972**, *14*, 299.
(32) Hudson, B. R.; Kohler, B. E. *J. Chem. Phys.* **1973**, *59*, 4984.
(33) Schulten, K.; Karplus, M. *Chem. Phys. Lett.* **1972**, *15*, 305.
(34) Simonetta, M.; Gianinetti, E.; Vandoni, I. *J. Chem. Phys.* **1968**, *48*, 1579.
(35) Schulten, K.; Ohmine, I.; Karplus, M. *J. Chem. Phys.* **1976**, *64*, 4422. Ohmine, I.; Karplus, M.; Schulten, K. *J. Chem. Phys.* **1978**, *68*, 2298.
(36) Tavan, P.; Schulten, K. *J. Chem. Phys.* **1986**, *85*, 6602.
(37) Tavan, P.; Schulten, K. *J. Chem. Phys.* **1979**, *70*, 5407.
(38) Zerbetto, F.; Zgierski, M. Z. *J. Chem. Phys.* **1990**, *93*, 1235.
(39) Aoyagi, M.; Ohmine, I.; Kohler, B. E. *J. Phys. Chem.* **1990**, *94*, 3922. Rossi, G.; Chance, R. R.; Silbey, R. *J. Chem. Phys.* **1989**, *90*, 7594.
(40) Granville, M. F.; Holtom, G. R.; Kohler, B. E. *J. Chem. Phys.* **1980**, *72*, 4671.
(41) Christensen, R. L.; Kohler, B. E. *J. Chem. Phys.* **1976**, *63*, 1837.
(42) Auerbach, R. A.; Christensen, R. L.; Granville, M. F.; Kohler, B. E. *J. Chem. Phys.* **1981**, *74*, 4.
(43) Simpson, J. H.; Mc Laughlin, L.; Scott Smith, D.; Christensen, R. L. *J. Chem. Phys.* **1987**, *87*, 3360.
(44) Kohler, B. E.; Spangler, C. S.; Westerfield, C. *J. Chem. Phys.* **1988**, *89*, 5422.
(45) Granville, M. F.; Kohler, B. E.; Snow, J. B. *J. Chem. Phys.* **1981**, *75*, 3765.
(46) Gavin, R. M., Jr.; Weisman, C.; McVey, J. K.; Rice, S. A. *J. Chem. Phys.* **1978**, *68*, 522.
(47) Girard, M.; Arvidson, E.; Christensen, R. *J. Chem. Phys.* **1984**, *80*, 2265.
(48) Andrews, J.; Hudson, B. S. *J. Chem. Phys.* **1978**, *68*, 4587.
(49) Granville, M. F.; Holtom, G. R.; Kohler, B. E.; Christensen, R. L.; D'Amico, K. *J. Chem. Phys.* **1979**, *70*, 593.
(50) Swofford, R. L.; McClain, W. M. *J. Chem. Phys.* **1973**, *59*, 5740.
(51) Holtom, G. R.; McClain, W. M. *Chem. Phys. Lett.* **1976**, *44*, 436.
(52) Bennett, J. A.; Birge, R. R. *J. Chem. Phys.* **1980**, *73*, 4234.
(53) Leopold, D. G.; Pendley, R. D.; Roebber, J. L.; Hemley, R. J.; Vaida, V. *J. Chem. Phys.* **1984**, *81*, 4218.
(54) Leopold, D. G.; Vaida, V.; Granville, M. F. *J. Chem. Phys.* **1984**, *81*, 4210.

(55) McDiarmid, R.; Doering, J. P. *Chem. Phys. Lett.* **1982**, *88*, 602.
(56) Doering, J. P.; McDiarmid, R. *J. Chem. Phys.* **1980**, *73*, 3617.
(57) McDiarmid, R.; Sabljic, A.; Doering, J. P. *J. Am. Chem. Soc.* **1985**, *107*, 826.
(58) Chadwick, R. R.; Gerrity, D. P.; Hudson, B. S. *Chem. Phys. Lett.* **1985**, *115*, 24.
(59) Buma, W. J.; Kohler, B. E.; Song, K. *J. Chem. Phys.* **1990**, *92*, 4622.
(60) Cave, R. J.; Davidson, E. R. *J. Phys. Chem.* **1987**, *91*, 4481.
(61) Cave, R. J.; Davidson, E. R. *Chem. Phys. Lett.* **1988**, *148*, 190.
(62) Cave, R. J.; Davidson, E. R. *J. Phys. Chem.* **1988**, *92*, 614.
(63) Cave, R. J.; Davidson, E. R. *J. Phys. Chem.* **1988**, *92*, 2173.
(64) Aoyagi, M.; Osamura, Y.; Iwata, S. *J. Chem. Phys.* **1985**, *83*, 1140.
(65) Nascimento, M. A. C.; Goddard, W. A., III, *Chem. Phys.* **1980**, *53*, 251.
(66) Bonacic-Koutecky, V.; Persico, M.; Dohnert, D.; Sevin, A. *J. Am. Chem. Soc.* **1982**, *104*, 6900.
(67) Szalay, P. G.; Karpten, A.; Lischka, H. *Chem. Phys.* **1989**, *130*, 219.
(68) Szalay, P. G.; Karpten, A.; Lischka, H. *Chem. Phys.* **1990**, *141*, 355.
(69) Kellogg, R. E.; Simpson, W. T. *J. Am. Chem. Soc.* **1965**, *87*, 4230.
(70) Minnaard, N. G.; Havinga, E. *Recl. Trav. Chim. Pays-Bas* **1973**, *92*, 1179.
(71) Allan, M.; Neuhaus, L.; Haselbach, E. *Helv. Chim. Acta* **1984**, *67*, 1776.
(72) Mosher, O. A.; Flicker, W. M.; Kuppermann, A. *J. Chem. Phys.* **1973**, *59*, 6502.
(73) Flicker, W. M.; Mosher, O. A.; Kuppermann, A. *Chem. Phys.* **1978**, *30*, 307.
(74) Doering, J. P. *J. Chem. Phys.* **1979**, *70*, 3902.
(75) Flicker, W. M.; Mosher, O. A.; Kuppermann, A. *Chem. Phys. Lett.* **1977**, *45*, 492.
(76) Dewar, M. J. S.; Zoebisch, E. G.; Healy, E. F.; Stewart, J. J. P. *J. Am. Chem. Soc.* **1985**, *107*, 3902.
(77) Warshel, A. In *Modern Theoretical Chemistry*; Schaefer, H. F., III, Ed.; Plenum: New York, 1977; Vol. 4, p 153.
(78) Warshel, A. *J. Chem. Phys.* **1975**, *62*, 214. Negri, F.; Orlandi, G.; Zerbetto, F. *J. Phys. Chem.* **1989**, *93*, 5124.
(79) Negri, F.; Orlandi, G. *J. Phys. Chem.* **1989**, *93*, 4470.
(80) Dinur, V.; Hemley, R. J.; Karplus, M. *J. Phys. Chem.* **1983**, *87*, 925.
(81) Kohler, B. E.; Spiglanin, T. S.; Hemley, R. J.; Karplus, M. *J. Chem. Phys.* **1984**, *80*, 23.
(82) Hemley, R. J.; Dinur, V.; Vaida, V.; Karplus, M. *J. Am. Chem. Soc.* **1985**, *107*, 836.
(83) Hemley, R. J.; Leopold, D. G.; Vaida, V.; Karplus, M. *J. Chem. Phys.* **1985**, *82*, 5379.
(84) Hemley, R. J.; Brooks, B. R.; Karplus, M. *J. Chem. Phys.* **1986**, *85*, 6550.
(85) Hemley, R. J.; Lasaga, A. C.; Vaida, V.; Karplus, M. *J. Phys. Chem.* **1988**, *92*, 945. Warshel, A.; Karplus, M. *Chem. Phys. Lett.* **1972**, *17*, 7.
(86) Zerbetto, F.; Zgierski, M. Z.; Orlandi, G. *Chem. Phys. Lett.* **1987**, *141*, 138.
(87) Zerbetto, F.; Zgierski, M. Z.; Negri, F.; Orlandi, G. *J. Chem. Phys.* **1988**, *89*, 4681.
(88) Negri, F.; Orlandi, G.; Zerbetto, F.; Zgierski, M. Z. *J. Chem. Phys.* **1989**, *91*, 6215.
(89) Negri, F.; Orlandi, G.; Brouwer, A. M.; Langkilde, F. W.; Wilbrandt, R. *J. Chem. Phys.* **1989**, *90*, 5944.
(90) Negri, F.; Orlandi, G.; Langkilde, F. W.; Wilbrandt, R. *J. Chem. Phys.* **1990**, *92*, 4907.
(91) Moeller, C.; Plesset, M. S. *Phys. Rev.* **1954**, *46*, 618.
(92) Das, G.; Wahl, A. C. *J. Chem. Phys.* **1972**, *56*, 1769.
(93) McWeeny, R.; Sutcliffe, B. T. *Comp. Phys. Rev.* **1985**, *2*, 217.
(94) Botschwina, P. *Chem. Phys. Lett.* **1974**, *29*, 98.
(95) Blom, C. E.; Altona, C. *Mol. Phys.* **1976**, *31*, 1377.
(96) Fogarasi, G.; Pulay, P.; Molt, K.; Sawodny, W. *Mol. Phys.* **1977**, *33*, 1565.
(97) Pulay, P.; Fogarasi, G.; Pongor, G.; Boggs, J. E.; Vargha, A. *J. Am. Chem. Soc.* **1983**, *105*, 7037.
(98) Shimanouchi, T. *Table of Molecular Vibrational Frequencies*; National Bureau of Standards: Washington, DC, 1972; Vol. 1.
(99) Cole, A. R.; Green, A. A.; Osborne, G. A. *J. Mol. Spectrosc.* **1973**, *48*, 212.
(100) Panchenko, Yu. N. *Spectrochim. Acta* **1975**, *31A*, 1201.
(101) Furukawa, Y.; Takeuchi, H.; Harada, I.; Tasumi, M. *Bull. Chem. Soc. Jpn.* **1983**, *56*, 392.
(102) Bock, C. W.; Panchenko, Yu. N.; Krasnoshchiokov, S. V.; Pupyshev, V. I. *J. Mol. Struct.* **1985**, *129*, 57.
(103) Bock, C. W.; McDiarmid, R.; Panchenko, Yu. N.; Pupyshev, V. I.; Krasnoshchiokov, S. V. *J. Mol. Struct.* **1990**, *222*, 415.
(104) Warshel, A.; Dauber, P. *J. Chem. Phys.* **1977**, *66*, 5477.
(105) Benedetti, E.; Aglietto, M.; Pucci, S.; Panchenko, Yu. N.; Pentin, Yu. A.; Nikitin, O. T. *J. Mol. Struct.* **1978**, *49*, 293.
(106) Huber-Walchli, P.; Gunthard, H. H. *Spectrochim. Acta* **1981**, *37A*, 285.
(107) McDiarmid, R.; Sheybani, A. H. *J. Chem. Phys.* **1988**, *89*, 1255.
(108) Abo Aly, M. M.; Baron, M. H.; Coulange, M. J.; Favrot, J. *Spectrochim. Acta* **1986**, *42A*, 411.
(109) Wilbrandt, R.; Langkilde, F. W. *Chem. Phys. Lett.* **1987**, *133*, 385.
(110) Abo Aly, M. M.; Baron, M. H.; Favrot, J.; Romain, F.; Revault, M. *Spectrochim. Acta* **1984**, *40A*, 1037.
(111) Lippincott, E. R.; White, C. E.; Sibilia, J. P. *J. Am. Chem. Soc.* **1982**, *84*, 3641.
(112) Rakovic, D.; Stepanyan, S. A.; Gribov, L. A.; Panchenko, Yu. N. *J. Mol. Struct.* **1982**, *90*, 363.
(113) Sabljic, A.; McDiarmid, R. *J. Chem. Phys.* **1985**, *82*, 2559. McDiarmid, R.; Sabljic, A. *J. Phys. Chem.* **1987**, *91*, 276.
(114) Langkilde, F. W.; Wilbrandt, R.; Faurskov Nielsen, O.; Hojgaard Christensen, D.; Nicolaisen, F. M. *Spectrochim. Acta* **1987**, *43A*, 1209.
(115) Fogarasi, G.; Liescheski, P. G.; Boggs, J. E. *J. Mol. Struct.* (THEOCHEM) **1987**, *151*, 341.
(116) Bock, C. W.; Panchenko, Yu. N.; Krasnoshchiokov, S. V.; Pupyshev, V. I. *J. Mol. Struct.* (THEOCHEM) **1986**, *148*, 131.
(117) Panchenko, Yu. N.; Rusach, E. B. *Moscow Univ. Chem. Bull.* **1979**, *34*, 221.
(118) Yoshida, H.; Tasumi, M. *J. Chem. Phys.* **1988**, *89*, 2803.
(119) Lippincott, E. R.; Feairheller, W. R.; White, C. E. *J. Am. Chem. Soc.* **1959**, *81*, 1316.
(120) Kohler, B. E.; Snow, J. B. *J. Chem. Phys.* **1983**, *79*, 2134.
(121) Squillacote, M. E.; Sheridan, R. S.; Chapman, O. L.; Anet, F. A. L. *J. Am. Chem. Soc.* **1979**, *101*, 3657.
(122) Lippincott, E. R.; Kenney, T. W. *J. Am. Chem. Soc.* **1962**, *84*, 3641.
(123) Panchenko, Yu. N.; Csaszar, P.; Torok, F. *Acta Chim. Hung.* **1983**, *113*, 149.
(124) Panchenko, Yu. N.; Pentin, Yu. A.; Rusach, E. B. *Russ. J. Phys. Chem.* **1975**, *49*, 2621.
(125) Ikeyama, T.; Azumi, T. *J. Chem. Phys.* **1982**, *76*, 5672.
(126) Hudson, B. S.; Loda, R. T. *Chem. Phys. Lett.* **1981**, *81*, 591.
(127) Noguchi, T.; Kolaczkowski, S.; Arbour, C.; Aramaki, S.; Atkinson, G. H.; Hayashi, H.; Tasumi, M. *Photochem. Photobiol.* **1989**, *50*, 603.
(128) Wunsch, L.; Neusser, H. J.; Schlag, E. W. *Chem. Phys. Lett.* **1975**, *31*, 433.
(129) Bray, R. G.; Hochstrasser, R. M.; Sung, N. H. *Chem. Phys. Lett.* **1975**, *33*, 1.
(130) Mikami, N.; Ito, M. *Chem. Phys.* **1977**, *23*, 141.
(131) Lichten, W. *Phys. Rev.* **1963**, *131*, 229. *Ibid.* **1967**, *164*, 31.
(132) Smith, F. T. *Phys. Rev.* **1969**, *179*, 111.
(133) O'Malley, T. F. *Advances in Atomic and Molecular Physics*; Academic: New York, 1971; Vol. 7.
(134) Herzberg, G.; Teller, E. *Z. Phys. Chem. (Leipzig)* **1933**, *21*, 410.
(135) Longuet-Higgins, H. C. *Advances in Spectroscopy*; Wiley-Interscience: New York, 1961; Vol. 2, p 429.
(136) Englman, R. *The Jahn–Teller Effect in Molecules and Crystals*, Wiley-Interscience: London, 1972.
(137) Orlandi, G.; Zerbetto, F. *Chem. Phys.* **1986**, *108*, 187.
(138) Del Bene, J.; Jaffé, H. H. *J. Chem. Phys.* **1968**, *48*, 1807.
(139) Orlandi, G. *Chem. Phys. Lett.* **1976**, *44*, 277.
(140) Zerbetto, F.; Zgierski, M. Z.; Orlandi, G.; Marconi, G. *J. Chem. Phys.* **1987**, *87*, 2505.
(141) Dushinsky, F. *Acta Physicochim. URSS*, **1937**, *1*, 551.
(142) Scharf, B.; Honig, B. *Chem. Phys. Lett.* **1970**, *7*, 132.
(143) Small, G. J. *J. Chem. Phys.* **1971**, *54*, 3300.
(144) Price, W. C.; Walsh, A. D. *Proc. R. Soc.* **1940**, *A174*, 220.
(145) Popow, E. M.; Kogan, G. A. *Opt. Spectrosc.* **1984**, *17*, 362.
(146) Gavin, R. M., Jr.; Risemberg, S.; Rice, S. A. *J. Chem. Phys.* **1973**, *58*, 3160.
(147) Peterson, N. O. *Can. J. Chem.* **1985**, *63*, 77.
(148) D'Amico, K. L.; Manos, C.; Christensen, R. L. *J. Am. Chem. Soc.* **1980**, *102*, 1777.
(149) Hennecker, W. H.; Siebrand, W.; Zgierski, M. Z. *J. Chem. Phys.* **1983**, *79*, 2495.
(150) Zerbetto, F.; Zgierski, M. Z. *Chem. Phys. Lett.* **1988**, *144*, 437.
(151) Su, W. P.; Schrieffer, J. R.; Heeger, A. J. *Phys. Rev.* **1983**, *B28*, 1138.
(152) Siebrand, W. In *Dynamics of Molecular Collisions*; Miller, W. H., Ed.; Plenum: New York, 1976; Part A. Jortner, J.; Rice, S. A.; Hochstrasser, R. M. *Adv. Photochem.* **1969**, *7*, 149.
(153) Saltiel, J.; D'Agostino, J. T.; Megarity, E. D.; Metts, L.; Neuberger, K. R.; Wrighton, M.; Zafirion, O. C. *Org. Photochem.* **1972**, *3*, 1.
(154) Gorman, A. A.; Gould, I. R.; Hamblett, I. *J. Am. Chem. Soc.* **1981**, *103*, 4553. Gorman, A. A.; Gould, I. R.; Hamblett, I. *J. Photochem.* **1982**, *19*, 89.
(155) Gorman, A. A.; Hamblett, I.; Irvine, M.; Raby, P.; Standen, M. C.; Yeates, S. *J. Am. Chem. Soc.* **1985**, *107*, 4404.

(156) Caldwell, R. A.; Singh, M. *J. Am. Chem. Soc.* **1982**, *104*, 6121.
(157) Kumar, C. V.; Chattopadhyay, S. K.; Das, P. K. *Chem. Phys. Lett.* **1984**, *106*, 431.
(158) Langkilde, F. W.; Wilbrandt, R.; Jensen, N.-H. *Chem. Phys. Lett.* **1984**, *111*, 372.
(159) Langkilde, F. W.; Jensen, N.-H.; Wilbrandt, R. *J. Phys. Chem.* **1987**, *91*, 1040.
(160) Birks, J. B. *Photophysics of Aromatic Molecules*; Wiley: London, 1970.
(161) Görner, H.; Schulte-Frohlinde, D. *J. Phys. Chem.* **1981**, *85*, 1835.
(162) Bonacic-Koutecky, V.; Ishimaru, S. *J. Am. Chem. Soc.* **1977**, *99*, 8134.
(163) Ohmine, I.; Morokuma, A. *J. Chem. Phys.* **1980**, *73*, 1907.
(164) Said, M.; Maynau, D.; Malrieu, J.-P. *J. Am. Chem. Soc.* **1984**, *106*, 580.
(165) Ohmine, I.; Morokuma, K. *J. Chem. Phys.* **1981**, *74*, 564.
(166) Zerbetto, F., unpublished.
(167) Wilbrandt, R.; Langkilde, F. W. *Chem. Phys. Lett.* **1987**, *133*, 385.
(168) Langkilde, F. W.; Jensen, N.-H.; Wilbrandt, R. *Chem. Phys. Lett.* **1985**, *118*, 486.
(169) Langkilde, F. W.; Jensen, N.-H.; Wilbrandt, R.; Brouwer, M. A.; Jacobs, H. J. C. *J. Phys. Chem.* **1987**, *91*, 1029.
(170) Wilbrandt, R.; Langkilde, F. W.; Brouwer, A. M.; Negri, F.; Orlandi, G. *J. Mol. Struct.* **1990**, *217*, 151.
(171) Negri, F.; Orlandi, G.; Langkilde, F. W.; Wilbrandt, R., in press.
(172) Jacobs, H. J. C.; Havinga, E. *Adv. Photochem.* **1979**, *11*, 305.
(173) Vroegop, P. J.; Lugtenburg, J.; Havinga, E. *Tetrahedron* **1973**, *29*, 1393.
(174) Hashimoto, H.; Koyama, Y.; Ichimura, K.; Kobayashi, T. *Chem. Phys. Lett.* **1989**, *162*, 523.
(175) Hashimoto, H.; Koyama, Y. *Chem. Phys. Lett.* **1989**, *162*, 523.
(176) Hashimoto, H.; Mukai, Y.; Koyama, Y. *Chem. Phys. Lett.* **1988**, *152*, 319.
(177) Mukai, Y.; Hashimoto, H.; Koyama, Y. *J. Phys. Chem.* **1990**, *94*, 4042.
(178) Mulliken, R. S.; Merer, A. J. *Chem. Rev.* **1969**, *69*, 639. Robin, M. B. *Higher Excited States of Polyatomic Molecules*; Academic: New York, 1975; Vol. 2, p 2; 1985; Vol. 3, p 213.
(179) Wilkinson, P. G.; Mulliken, R. S. *J. Chem. Phys.* **1955**, *23*, 1895.
(180) Foo, P. D.; Innes, K. K. *J. Chem. Phys.* **1974**, *60*, 4582.
(181) McDiarmid, R.; Charney, E. *J. Chem. Phys.* **1967**, *47*, 1517.
(182) McDiarmid, R. *J. Chem. Phys.* **1969**, *50*, 1794.
(183) Merer, A. J.; Schoonveld, L. *Can. J. Phys.* **1969**, *47*, 1731.
(184) Wilden, D. G.; Comer, J. *J. Phys. B* **1979**, *12*, L371. *Ibid.* **1980**, *13*, 1009.
(185) Evans, D. F. *J. Chem. Soc.* **1960**, 1735.
(186) McDiarmid, R. *J. Chem. Phys.* **1971**, *55*, 4669.
(187) Siebrand, W.; Zgierski, M. Z. *Chem. Phys.* **1980**, *52*, 321.
(188) Buenker, R. J.; Peyerimhoff, S. D.; Hsu, H. L. *Chem. Phys. Lett.* **1971**, *11*, 65.
(189) Petrongolo, C.; Buenker, R. J.; Peyerimhoff, S. D. *J. Chem. Phys.* **1982**, *76*, 3655.
(190) Petrongolo, C.; Buenker, R. J.; Peyerimhoff, S. D. *J. Chem. Phys.* **1983**, *78*, 7284.
(191) Yamaguchi, Y.; Osamura, Y.; Schaefer, H. F., III *J. Am. Chem. Soc.* **1983**, *105*, 7506.
(192) Siebrand, W.; Zerbetto, F.; Zgierski, M. Z. *J. Chem. Phys.* **1989**, *91*, 5926.
(193) Siebrand, W.; Zerbetto, F.; Zgierski, M. Z. *Chem. Phys. Lett.* **1990**, *174*, 119.
(194) Dupuis, M.; Spangler, D.; Wendoloski, J. J. *NRCC* Software Catalog, Program QG01, Lawrence Berkeley, Laboratory, Livermore, CA 1980.
(195) Clark, T.; Chandrasekhar, J.; Spitznagel, G. W.; Schleyer, P. v. R. *J. Comput. Chem.* **1983**, *4*, 294.
(196) Frisch, M. J.; Pople, J. A.; Binkley, J. S. *J. Chem. Phys.* **1984**, *80*, 3265.
(197) Dupuis, M.; Watts, J. D.; Villar, H. O.; Hurst, G. J. B. HONDO7.0. *QCPE* No. 544, **1987**.
(198) Wallace, R. *Chem. Phys. Lett.* **1989**, *159*, 35.
(199) Sension, R. J.; Hudson, B. S. *J. Chem. Phys.* **1989**, *90*, 1377.
(200) Duncan, J. L.; Hamilton, E. *J. Mol. Struct.* **1981**, *76*, 65.
(201) Siebrand, W.; Zgierski, M. Z. *J. Mol. Struct.* **1991**, *242*, 61.
(202) McDiarmid, R. *J. Phys. Chem.* **1980**, *84*, 64.
(203) Sension, R. J.; Mayne, L.; Hudson, B. S. *J. Am. Chem. Soc.* **1987**, *109*, 5036.
(204) Merer, A. J.; Watson, J. K. G. *J. Mol. Spectrosc.* **1973**, *47*, 499.
(205) Jones, L. C., Jr.; Taylor, L. W. *Anal. Chem.* **1955**, *27*, 228.
(206) Suzuki, H. *Electronic Absorption Spectra and Geometry of Organic Molecules*; Academic Press: New York, 1967.
(207) McDiarmid, R. *J. Chem. Phys.* **1976**, *64*, 514.
(208) Hemley, R. J.; Dawson, J. I.; Vaida, V. *J. Chem. Phys.* **1983**, *78*, 2915.
(209) Zerbetto, F.; Zgierski, M. Z. *Chem. Phys. Lett.* **1989**, *157*, 515.
(210) Petelenz, P.; Petelenz, B. *J. Chem. Phys.* **1975**, *62*, 3482.
(211) Myers, A. B.; Pranata, K. S. *J. Phys. Chem.* **1989**, *93*, 5079.
(212) Ci, X.; Pereira, M. A.; Myers, A. B. *J. Chem. Phys.* **1990**, *92*, 4708.
(213) Henneker, W. H.; Siebrand, W.; Zgierski, M. Z. *Chem. Phys. Lett.* **1979**, *68*, 5.
(214) Heimbrook, L. A.; Kenny, J. E.; Kohler, B. E.; Scott, G. W. *J. Chem. Phys.* **1981**, *75*, 4338.
(215) Kohler, B. E.; Spiglanin, T. A. *J. Chem. Phys.* **1984**, *80*, 3091.
(216) Birge, R. R. *Annu. Rev. Biophys. Bioeng.* **1981**, *10*, 315.
(217) Birge, R. R.; Bocian, D. F.; Hubbard, L. M. *J. Am. Chem. Soc.* **1982**, *104*, 1196.
(218) Christensen, R. L.; Kohler, B. E. *Photochem. Photobiol.* **1973**, *18*, 293.
(219) Warshel, A.; Karplus, M. *J. Am. Chem. Soc.* **1974**, *96*, 5677.
(220) Honig, B.; Warshel, A.; Karplus, M. *Acc. Chem. Res.* **1975**, *8*, 92.
(221) Myers, A. B.; Trulson, M. O.; Pardoen, J. A.; Heeremans, C.; Lugtenburg, J.; Mathies, R. A. *J. Chem. Phys.* **1986**, *84*, 633.
(222) Inagaki, F.; Tasumi, M.; Miyazawa, T. *J. Mol. Spectrosc.* **1974**, *50*, 386.
(223) Siebrand, W.; Zgierski, M. Z. *J. Chem. Phys.* **1979**, *71*, 3561.
(224) Iqbal, Z.; Weidekamm, E. *Biochim. Biophys. Acta* **1977**, *555*, 426.
(225) Hashimoto, H.; Koyama, Y. *Chem. Phys. Lett.* **1989**, *154*, 321.
(226) Heeger, A. J.; Kivelson, S.; Schrieffer, J. R.; Su, W. P. *Rev. Mod. Phys.* **1988**, *60*, 781.
(227) Soos, Z. G.; Hayden, G. W. *Electroresponsive Molecular and Polymeric Systems*; Skotheim, T., Ed.; Dekker: New York, 1988; Vol. 1, p 197.
(228) Cataliotti, R. S.; Paliani, G.; Dellepiane, G.; Fuso, S.; Destri, S.; Piseri, L.; Tubino, R. *J. Chem. Phys.* **1985**, *82*, 2223.
(229) Lichtmann, L. S.; Imhoff, E. A.; Sarhangi, A.; Fitchen, D. B. *J. Chem. Phys.* **1984**, *81*, 168.
(230) Lichtmann, L. S.; Sarhangi, A.; Fitchen, D. B. *Solid State Commun.* **1981**, *36*, 869.
(231) Fitchen, D. B. *Mol. Cryst. Liquid Cryst.* **1982**, *83*, 95.
(232) Mulazzi, E.; Brivio, G. P.; Faulques, E.; Lefrant, S. *Solid State Commun.* **1983**, *46*, 841.
(233) Siebrand, W.; Zgierski, M. Z. *J. Chem. Phys.* **1984**, *81*, 185.
(234) Tarr, A. W.; Siebrand, W. *J. Raman Spectrosc.* **1989**, *20*, 209.
(235) Fuso, S.; Cuniberti, C.; Piaggio, P.; Dellepiane, G.; Luzzati, S.; Tubino, R.; Zgierski, M. Z. *J. Chem. Phys.* **1987**, *87*, 6816.
(236) Saito, S.; Tasumi, M.; Eugster, C. H. *J. Raman Spectrosc.* **1983**, *14*, 299.
(237) Snyder, R.; Arvidson, E.; Foote, C.; Harrigan, L.; Christensen, R. L. *J. Am. Chem. Soc.* **1985**, *107*, 4117.
(238) Birks, J. B.; Dyson, D. J. *Proc. R. Soc. London* **1963**, *A275*, 135.
(239) Cehelnik, E. D.; Cundall, R. B.; Lockwood, J. R.; Palmer, T. F. *J. Phys. Chem.* **1975**, *79*, 1369.
(240) Song, P. S.; Chae, Q.; Fuijta, M.; Hiroaki, B. *J. Am. Chem. Soc.* **1976**, *98*, 819.
(241) Mortensen, O. S.; Siebrand, W.; Tarr, A. W. *Chem. Phys.* **1988**, *125*, 231.
(242) Wasilewski, M. R.; Johnson, D. G.; Bradford, E. G.; Kispert, L. D. *J. Chem. Phys.* **1989**, *91*, 6691.
(243) Siebrand, W. *J. Chem. Phys.* **1967**, *47*, 2411.
(244) Lawetz, V.; Siebrand, W.; Orlandi, G. *Chem. Phys. Lett.* **1972**, *16*, 448.
(245) Avouris, P.; Gelbart, W. M.; El-Sayed, M. A. *Chem. Rev.* **1977**, *77*, 793.
(246) Siebrand, W.; Zgierski, M. Z. *Chem. Phys. Lett.* **1980**, *72*, 411.
(247) Siebrand, W.; Zgierski, M. Z. *J. Chem. Phys.* **1981**, *75*, 1230.
(248) Hudson, B. S.; Andrews, J. *Chem. Phys. Lett.* **1979**, *63*, 493.
(249) Zerbetto, F. Doctoral dissertation, Bologna, 1986.
(250) Zerbetto, F.; Zgierski, M. Z. *Chem. Phys.* **1988**, *127*, 17.
(251) Pulay, P. *Mol. Phys.* **1960**, *17*, 197.